« ARCO 11831 layout: Large reference style: basic file: arco9004.tex (Aistes) aid: 9004 doctopic: OriginalPaper class: spr-twocol-v1 v.2007/05/18 Prn:19/05/2007; 13:34 p. 1»

Arch Comput Methods Eng
DOI 10.1007/s11831-007-9004-8

A Fluid-Dynamic Traffic Model on Road Networks

Gabriella Bretti · Roberto Natalini · Benedetto Piccoli

Received: 13 April 2006 / Accepted: 13 March 2007

Abstract We consider a mathematical model for fluid-dynamic flows on networks which is based on conservation laws. Road networks are studied as graphs composed by arcs that meet at some nodes, corresponding to junctions, which play a key-role. Indeed interactions occur at junctions and there the problem is underdetermined. The approximation of scalar conservation laws along arcs is carried out by using conservative methods, such as the classical Godunov scheme and the more recent discrete velocities kinetic schemes with the use of suitable boundary conditions at junctions. Riemann problems are solved by means of a simulation algorithm which processes each junction. We present the algorithm and its application to some simple test cases and to portions of urban network.

1 Introduction

The study of traffic flow aims to understand traffic behaviour in urban context in order to answer to several questions: where to install traffic lights or stop signs; how long the cycle of traffic lights should be; where to construct entrances, exits, and overpasses. The purposes of this analysis are principally represented by the maximization of cars flow, and the minimization of traffic congestions, accidents and pollution. In general, network models of transportation systems are assumed to be static, but these models do not allow a correct simulation of heavily congested urban road networks. For this reason, traffic engineers have started to consider some alternative models, often referred to as DTA (dynamic traffic assignment) or *within-day* models, see the review paper [3] and references therein. The use of within-day modelling makes necessary to give a new formulation of the problem: we have to solve the DNL (dynamic network loading) problem, that is, the reproduction of the traffic flow motion on the network, which requires the introduction of time advancing mathematical models (traffic simulation models). However, the main problems in DNL models are the fact that they do not properly reproduce the backward propagation of shocks and the difficulty of collecting experimental data to test the models.

Microscopic models, which form a widely used class of models, are characterized by the fact that they are sensitive to small perturbations. On the other hand, it can be difficult to give a qualitative description and visualization of phenomena on a macroscopic scale.

Here we deal with the fluid-dynamic models proposed in [8, 9], which can be seen as a macroscopic model with some traffic regulation strategies (within-day models) and which allows to observe the network in the time evolution through waves formation. In the 1950s James Lighthill and Gerald Whitham in [20], and independently Richards in [24], proposed to apply fluid dynamics concepts to traffic. In a single road, this nonlinear model is based on the conservation of cars described by the scalar hyperbolic conservation law:

$$\partial_t \rho + \partial_x f(\rho) = 0, \tag{1.1}$$

G. Bretti (✉)
Department of Information Engineering and Applied Mathematics, University of Salerno, via Ponte don Melillo, 84084 Fisciano (SA), Italy
e-mail: g.bretti@iac.cnr.it

R. Natalini · B. Piccoli
Istituto per le Applicazioni del Calcolo "M. Picone" Viale del Policlinico 137, 00161 Rome, Italy

R. Natalini
e-mail: r.natalini@iac.cnr.it

B. Piccoli
e-mail: b.piccoli@iac.cnr.it

where $\rho = \rho(t,x) \in [0, \rho_{\max}]$ is the density of cars, $(t,x) \in \mathbb{R}^2$ and $\rho_{\max} > 0$ is the maximum density of cars on the road. The function $f(\rho)$ is the flux of cars, which is written as product of the density and of the local speed of cars v: i.e. $f(\rho) = \rho v$. In most cases, and at least as a first order approximation, one can assume that v is a decreasing function, only depending on the density, and that the corresponding flux is a concave function. We refer to [14, 25] for more details and comments on the single road models. Let us remark that fluid-dynamic models for traffic flow seem to be the most appropriate to detect macroscopic phenomena as shocks formation and propagation of waves backwards along roads. However, they can develop discontinuities in a finite time even starting from smooth initial data, then needing for a careful definition of the analytical framework, and an even greater consideration of suitable numerical schemes. We refer to [5, 10] for an updated account of the theory of general hyperbolic conservation laws, and to [12, 19] for a standard introduction to the main numerical ideas. Notice that, in all this classical works on traffic flows, only a single road was taken into account. More recently, in [8, 9, 16, 18], some models have been proposed for traffic flow on road networks. Following [9], we focus on a road network composed by a finite number of roads parametrized by intervals $[a_i, b_i]$ that meet at some junctions. Junctions play a key role, as the system at a junction is underdetermined even after prescribing the conservation of cars, that can be written as the Rankine-Hugoniot condition:

$$\sum_{i=1}^{n} f(\rho_i(t,b_i)) = \sum_{j=n+1}^{n+m} f(\rho_j(t,a_j)),$$

where ρ_i, $i = 1,\dots,n$, are the car densities on incoming roads; ρ_j, $j = n+1,\dots,n+m$, are the car densities on outgoing roads. Such relation expresses the equality of ingoing and outgoing fluxes. For endpoints that do not touch a junction (and are not infinite), we assume to have a given boundary data and solve the corresponding boundary problem, as in [4]. Let us remark that, in this paper, traffic lights will not be considered, since their analytical and numerical theory is already well understood [25].

As in [9], we make the following two assumptions: there are some distribution coefficients of traffic from incoming roads to outgoing roads; drivers behave in such a way to maximize fluxes whenever is possible. One could also treat junctions where the number of incoming roads is greater than the number of outgoing ones, not covered by the analysis of [9]. In particular, we are interested in the case of two incoming and one outgoing roads. In this case, the two distribution coefficients of the incoming roads must be equal to one, thus determining a loss of uniqueness for the solutions. This is not a purely mathematical issue, but it is rather due to the fact that if not all cars can go through the junction then there should be a yielding rule between incoming roads. To treat this case we introduce a new parameter $q \in]0,1[$, the *right of way* (see [8]), which permits to uniquely solve Riemann problems. In particular, it indicates which, among cars passing through the junction, is the percentage of cars coming from the first incoming road and which is the percentage coming from the second road. The details about the mentioned rules are discussed in Sect. 2.

We deal with the numerical approximation of the possibly discontinuous solutions produced by this model. In particular, the main contribution of the paper is represented by the introduction of suitable boundary conditions at the junctions for classical and less classical numerical schemes. These schemes, namely Godunov scheme and Kinetic methods, adapted to the problem, provide approximations which are quite stable as we will show later through many numerical tests.

The paper is organized as follows. Section 2 is devoted to the description of the model. Some examples of simple networks are proposed in Sect. 2.4. In Sect. 3 we describe the numerical schemes with the particular boundary conditions used to produce approximated solutions of the problem. In Sect. 4 we give an extended presentation of some numerical experiments which show the effectiveness of our approximation.

2 Backgrounds

We consider the conservation of cars described by the equation [20, 24]:

$$\partial_t \rho + \partial_x f(\rho) = 0, \tag{2.1}$$

where $\rho = \rho(t,x)$ is the density of cars, with $\rho \in [0, \rho_{\max}]$, $(t,x) \in \mathbb{R}^2$ and $\rho_{\max}$ is the maximum density of cars on the road; $f(\rho)$ is the flux, which can be written $f(\rho) = \rho v(\rho)$, with $v(t,x)$ the velocity. Typically v is a smooth decreasing function of ρ.

2.1 Traffic Variables: Velocity, Flow and Density

Equation (2.1) is the consequence of conservation of cars and experimental relationships between car velocity and traffic density.

2.1.1 *Velocity Field*

Let us consider a car moving along a highway. There are two ways to measure velocity. The most common is to record the velocity $v_i = \frac{dx_i}{dt}$ of each car. With N cars there are different velocities, $v_i(t)$, $i = 1,\dots,N$, each depending on time. If the number of cars N is large, it becomes difficult to keep track of each car. So, instead of measuring the velocity of

« **ARCO 11831** layout: Large reference style: basic file: arco9004.tex (Aistes) aid: 9004 doctopic: OriginalPaper class: spr-twocol-v1 v.2007/05/18 Prn:19/05/2007; 13:34 p. 3»

each individual car, we associate to each point in space at each time a *velocity field*, $v(x,t)$. This would be the velocity measured by an observer fixed at position x at time t.

2.1.2 Traffic Flow and Traffic Density

In addition to car velocities, an observer fixed at a certain position along the highway, could measure the number of cars that passed in a given length of time. The average number of cars passing per time unit (for example one minute) is called the *traffic flow* $f = f(x,t)$.

A systematic procedure could be employed to take into account cars completely in a given region at a fixed time; estimates of fractional cars could be used or a car could be counted only if its center is in the region. These measurements give the *density* of cars, ρ, that represents the number of cars per distance unit (for example hundred of meters).

2.1.3 Flow Equals Density Times Velocity

There is a close relationship between the three fundamental traffic variables: velocity, density and flow. It is quite realistic to think to the flux f—the number of cars per time unit—as a function of the only density ρ. More precisely the flux will be expressed as

$$\boxed{f(x,t) = \rho(x,t)v(x,t),} \tag{2.2}$$

that means

$$\boxed{\text{traffic flow} = (\text{traffic density}) \times (\text{mean velocity}).}$$

As the density increases (meaning there are more and more cars per meter), the velocity of cars diminishes. Thus we make the hypothesis that the velocity of cars at any point of the road is a regular strictly decreasing function of the density:

$$\boxed{v = v(\rho).}$$

Lighthill and Whitham and independently Richards in the mid-1950 s proposed this type of mathematical model of traffic flow.

If there are no other cars on the highway (corresponding to very low traffic densities), then the car would travel at the maximum speed $v_{\max}$, sometimes referred to as the "mean free speed":

$$v(0) = v_{\max}.$$

At a certain density cars stop before they touch to each other. This maximum density, $\rho_{\max}$, usually corresponds to what is called bumper-to-bumper traffic:

$$v(\rho_{\max}) = 0.$$

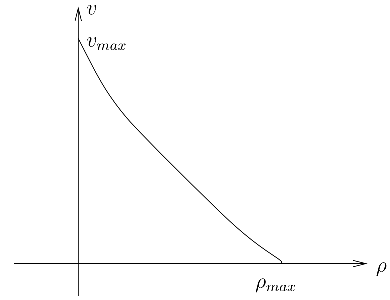

2.1.4 Conservation of the Number of Cars

Let us fix a certain segment (a,b) on the highway and two quite close times $t_1 < t_2$. We are assuming that no cars are created or destroyed in the interval, then the changes in the number of cars result from crossings at $x = a$ and $x = b$ only. We deduce that the cars entered from the point a at a certain time will exit from the point b. Thus the difference of the total quantity of cars in the segment between the two considered instants

$$\int_a^b \rho(x,t_2)dx - \int_a^b \rho(x,t_1)dx$$

must be equal to the difference of the total flux at the endpoints

$$\int_{t_1}^{t_2} f(a,t)dt - \int_{t_1}^{t_2} f(b,t)dt.$$

Dividing the integrals for the product of $b-a$ and $t_2 - t_1$ and taking the limits $(b-a) \to 0$ and $(t_2 - t_1) \to 0$, with the assumption that v and f are regular, we finally obtain the conservation law:

$$\rho_t + f_x = 0. \tag{2.3}$$

Taking the velocity as

$$v(\rho) = v_{\max}\left(1 - \frac{\rho}{\rho_{\max}}\right),$$

we have the flux

$$f(\rho) = v_{\max}\left(1 - \frac{\rho}{\rho_{\max}}\right)\rho.$$

The flux is null if there are no cars or if the density is maximum and it reaches the maximum for $\rho = \frac{\rho_{\max}}{2}$. It is easy to see the presence of discontinuity if someone brakes. The density assumes a discontinuity that propagates backwards along the queue.

For further details see [14].

2.2 Basic Definitions for Road Networks

For the notions about the model given in the sequel we refer to the paper by Piccoli and coauthors [9].

Different types of mathematical models can be used for the simulation of vehicular traffic. They can be roughly classified in microscopic, mesoscopic and macroscopic. The basic models are the car following or microscopic models based on Newton's law. The macroscopic models seem to properly treat some phenomena such as shocks creation and propagation. Here we propose a fluid-dynamic model for traffic flow on a road network, which can be applied to the case of crossings with lights and circles. We consider the conservation law formulation proposed by Lighthill-Whitham and Richards. More precisely, one considers the conservation of cars described by (2.1), where $\rho = \rho(x,t)$ is the density of cars, with $\rho \in [0, \rho_{\max}]$, $(x,t) \in \mathbb{R}^2$ and $\rho_{\max}$ is the maximum density of cars on the road; $f(\rho)$ is the flux, which can be written $f(\rho) = \rho v(\rho)$, with $v(x,t)$ the velocity. Typically v is assumed to be a smooth decreasing function of ρ.

Here we are interested in a road network. This means that we have a finite number of roads modelled by intervals $[a_i, b_i]$ (with one of the endpoints eventually infinite) that meet at the some junctions. We give boundary data and solve the associated boundary problem for the endpoints (not infinite) that do not meet at any junction. Junctions play a fundamental role, as the system at a junction is underdetermined, even after prescribing the conservation of cars. The Rankine-Hugoniot at a junction reads:

$$\sum_{i=1}^{n} f(\rho_i(t, b_i)) = \sum_{j=n+1}^{n+m} f(\rho_j(t, a_j)),$$

where ρ_i, $i = 1, \dots, n$, are the car densities on incoming roads; ρ_j, $j = n+1, \dots, n+m$, are the car densities on the outgoing roads.

To determine a unique solution to Riemann problems at junctions, assume the following criteria:

(A) there are some fixed coefficients, the prescribed preferences of drivers, that express the distribution of traffic from incoming to outgoing roads;
(B) respecting (A), drivers choices are made in order to maximize the flux.

Let us consider the rule (A). We fix a matrix, called *traffic distribution matrix*:

$$A = \{\alpha_{ji}\}_{j=n+1,\dots,n+m, i=1,\dots,n} \in \mathbb{R}^{m \times n},$$

such that

$$0 < \alpha_{ji} < 1, \qquad \sum_{j=n+1}^{n+m} \alpha_{ji} = 1, \tag{2.4}$$

for $i = 1, \dots, n$ and $j = n+1, \dots, n+m$, where α_{ji} is the percentage of drivers arriving from the i-th incoming road that take the j-th outgoing road.

Remark 2.1 Note that the only the rule (A) is not sufficient to have a unique solution to Riemann problems, that are still under-determined.

Under suitable assumptions on A and rules (A)–(B), representing a situation where drivers have a final destination and maximize the flux whenever is possible, Riemann problems can be uniquely solved. In [9] it has been proved existence of each solution to Cauchy problems respecting rules (A) and (B).

It is possible to introduce time dependent coefficients for the rule (A), and in particular traffic lights are modelled to deal with periodic coefficients. In the same way, we can treat networks assigning a different flux function f_i on each road I_i.

Let us first recall the basic definitions and results from [9]. The parametrization of roads composing a network is made through a set of intervals $I_i = [a_i, b_i] \subset \mathbb{R}$, $i \in 1, \dots, N$, with the endpoints possibly infinite. The datum is a finite collection of densities ρ_i defined on $I_i \times [0, +\infty)$.

ρ_i is a weak entropy solution on road I_i, if for every $\varphi : I_i \to \mathbb{R}$ smooth and with compact support on $(a_i, b_i) \times (0, +\infty)$ one has

$$\int_{a_i}^{b_i} \int_0^{+\infty} \left(\rho_i \frac{\partial \varphi}{\partial t} + f(\rho_i) \frac{\partial \varphi}{\partial x} \right) dx\,dt = 0 \tag{2.5}$$

and for every $k \in \mathbb{R}$ and $\tilde{\varphi} : I_i \to \mathbb{R}$ smooth, positive with compact support on $(a_i, b_i) \times (0, +\infty)$

$$\int_{a_i}^{b_i} \int_0^{+\infty} \Bigg(|\rho_i - k| \frac{\partial \tilde{\varphi}}{\partial t} + \operatorname{sgn}(\rho_i - k)(f(\rho_i) - f(k)) \frac{\partial \tilde{\varphi}}{\partial x} \Bigg) dx\,dt \ge 0. \tag{2.6}$$

For (2.1) on $\mathbb{R}$ it is well-known that there exists a unique weak entropy solution for every initial data belonging to L^∞, with a continuous dependence on the initial data in L^1_{loc}. Roads are linked to each other by some junctions, with the assumption that each road can be incoming at most for one junction and outgoing at most for one junction. Consequently the complete model is given by a pair $(\mathcal{I}, \mathcal{J})$, with $\mathcal{I} = \{I_i : i = 1, \dots, N\}$ the collection of roads and $\mathcal{J}$ the number of junctions.

Consider a junction J with n incoming roads, say $I_1, \dots, I_n$, and m outgoing roads, say $I_{n+1}, \dots, I_{n+m}$. A *weak solution at the junction* J is a collection of functions $\rho_l : [0, +\infty[\times I_l \to \mathbb{R}$, $l = 1, \dots, n+m$, such that

$$\sum_{l=0}^{n+m} \left(\int_0^{+\infty} \int_{a_l}^{b_l} \left(\rho_l \frac{\partial \varphi_l}{\partial t} + f(\rho_l) \frac{\partial \varphi_l}{\partial x} \right) dx\,dt \right) = 0, \tag{2.7}$$

« ARCO 11831 layout: Large reference style: basic file: arco9004.tex (Aistes) aid: 9004 doctopic: OriginalPaper class: spr-twocol-v1 v.2007/05/18 Prn:19/05/2007; 13:34 p. 5»

for every φ_l, $l = 1, \ldots, n+m$, smooth having compact support in $(0, +\infty) \times (a_l, b_l]$ for $l = 1, \ldots, n$ (incoming roads) and in $(0, +\infty) \times [a_l, b_l)$ for $l = n+1, \ldots, n+m$ (outgoing roads), that are also *smooth across the junction*, i.e.

$$\varphi_i(b_i, \cdot) = \varphi_j(a_j, \cdot), \qquad \frac{\partial \varphi_i}{\partial x}(b_i, \cdot) = \frac{\partial \varphi_j}{\partial x}(a_j, \cdot),$$
$$i = 1, \ldots, n, \; j = n+1, \ldots, n+m.$$

Remark 2.2 Let $\rho = (\rho_1, \ldots, \rho_{n+m})$ be a weak solution at the junction such that each $x \to \rho_i(t, x)$ has bounded variation. We can deduce that ρ satisfies the *Rankine-Hugoniot Condition* at the junction J, namely

$$\sum_{i=1}^{n} f(\rho_i(b_i-, t)) = \sum_{j=n+1}^{n+m} f(\rho_j(a_j+, t)), \tag{2.8}$$

for almost every $t > 0$.

The rules (A) and (B) can be given explicitly only for solutions with bounded variation as in the next definition.

Definition 2.3 Let $\rho = (\rho_1, \ldots, \rho_{n+m})$ be such that $\rho_i(x, t)$ is of bounded variation for every $t \geq 0$. Then ρ is an admissible weak solution of (2.1) associated to the matrix A, satisfying (2.4), at the junction J the following properties hold:

(i) ρ is a weak solution at the junction;
(ii) $f(\rho_j(a_j^+, \cdot)) = \sum_{i=1}^{n} \alpha_{ji} f(\rho_i(b_i^+, \cdot))$, for $j = n+1, \ldots, n+m$;
(iii) $f(\rho_i(b_i^-, \cdot)) + \sum_{j=n+1}^{n+m} f(\rho_j(a_j^+, \cdot))$, is maximum subject to (ii).

A boundary data $\psi_i : [0, +\infty] \to \mathbb{R}$ is assigned in the following cases: for each road $I_i = [a_i, b_i]$, if $a_i > -\infty$ and I_i is not the outgoing road of any junction, or if $b_i < +\infty$ and I_i is not the incoming road of any junction. If boundary data is given, we need ϕ_i to verify $\rho_i(a_i, t) = \psi_i(t)$ or $\rho_i(b_i, t) = \psi_i(t)$ in the sense of [4].

Definition 2.4 Given $\bar{\rho}_i : I_i \to \mathbb{R}$ and possibly $\psi_i : [0, +\infty[\to \mathbb{R}$, functions of L^∞, a collection of functions $\rho = (\rho_1, \ldots, \rho_N)$ with $\rho_i : [0, +\infty[\times I_i \to \mathbb{R}$ continuous as functions from $[0, +\infty[$ into L^1_{loc}, is an admissible solution if ρ_i is a weak entropy solution to (2.1) on I_i, $\rho_i(x, 0) = \bar{\rho}_i(x)$ a.e., $\rho_i(b_i, t) = \psi_i(t)$ in the sense of [4], finally such that at each junction ρ is a weak solution and is an admissible weak solution in case of bounded variation.

We recall the construction of solutions to the Riemann problems for rules (A) and (B). A Riemann problem for a scalar conservation law is a Cauchy problem for an initial data of Heaviside type, that is piecewise constant with only one discontinuity. Once Riemann problems are solved, a solution to Cauchy problems can be obtained, for instance, by wave front tracking. In case of concave or convex fluxes, the Riemann solutions are of two types: continuous waves called rarefactions and travelling discontinuities called shocks. The speed of the waves is related to $f'(\rho)$.

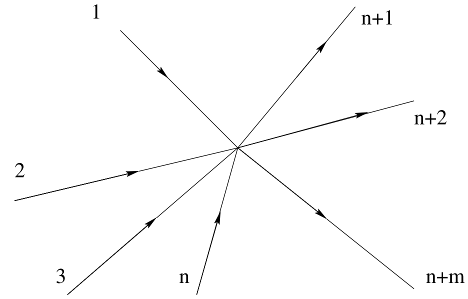

Fig. 1 Junction

For a junction, as for a scalar conservation law, a Riemann problem is a Cauchy problem with an initial data that is constant on each road. Let us make the subsequent assumptions on the flux:

($\mathcal{F}$) $f : [0, 1] \to \mathbb{R}$ is smooth, strictly concave (i.e. $f'' \leq -c < 0$ for some $c > 0$), $f(0) = f(1) = 0$, $|f'(x)| \leq C < +\infty$. Hence there exists a unique $\sigma \in]0, 1[$ such that $f'(\sigma) = 0$ (that is σ is a strict maximum).

Consider a junction J with n incoming roads and m outgoing roads. The densities of cars on the incoming roads are indicated by:

$$(x, t) \in \mathbb{R}^+ \times I_i \mapsto \rho_i(x, t) \in [0, 1], \quad i \in \{1, \ldots, n\}$$

and those on the outgoing roads:

$$(x, t) \in \mathbb{R}^+ \times I_j \mapsto \rho_j(x, t) \in [0, 1], \quad j \in \{1, \ldots, m\}.$$

We introduce the following application:

Definition 2.5 Let $\tau : [0, 1] \mapsto [0, 1]$, $\tau(\sigma) = \sigma$, be the map satisfying the following

$$\tau(\rho) \neq \rho, \qquad f(\tau(\rho)) = f(\rho),$$

for each $\rho \neq \sigma$.

Evidently τ is well-defined and it verifies

$$0 \leq \rho \leq \sigma \Longleftrightarrow \sigma \leq \tau(\rho) \leq 1,$$
$$\sigma \leq \rho \leq 1 \Longleftrightarrow 0 \leq \tau(\rho) \leq \sigma.$$

In order to ensure uniqueness of the solution to Riemann problems we need some generic additional conditions on the matrix A. Let $\{e_1, \ldots, e_n\}$ be the canonical basis of $\mathbb{R}^n$ and for every subset $V \subset \mathbb{R}^n$, indicate by $V^\perp$ its orthogonal. For every $i = 1, \dots, n$, let us define H_i the coordinate hyperplane orthogonal to e_i and for every $j = n+1, \dots, n+m$ define $H_j = {\alpha_j}^{\perp}$, with $\alpha_j = (\alpha_{j1}, \dots, \alpha_{jn})$. Indicate by $\mathcal{K}$ the set of indices $k = (k_1, \dots, k_l)$, $1 \le l \le n-1$, such that $0 \le k_1 < k_2 < \cdots < k_l \le n+m$ and for every $k \in \mathcal{K}$ we set

$$H_k = \bigcap_{h=1}^{l} H_{k_h}.$$

Letting $\mathbf{1} = (\mathbf{1}, \dots, \mathbf{1}) \in \mathbb{R}^{\mathbf{n}}$, we assume

(RP) For every $k \in \mathcal{K}$, $\mathbf{1} \notin \mathbf{H}_{\mathbf{k}}^{\perp}$.

From (RP) easily follows $m \ge n$, for the details see [9].

The existence and uniqueness of admissible solutions for the Riemann problem of a junction is expressed by the next theorem.

Theorem 2.6 *Let $f : [0,1] \to \mathbb{R}$ satisfy $(\mathcal{F})$, the matrix A satisfy (C) and $\rho_{1,0}, \dots, \rho_{n+m,0} \in [0,1]$ be constants. There exists a unique admissible weak solution, in the sense of Definition 2.3, namely $\rho = (\rho_1, \dots, \rho_{n+m})$ of (2.1) at the junction J such that*

$$\rho_1(0,\cdot) \equiv \rho_{1,0}, \dots, \rho_{n+m}(0,\cdot) \equiv \rho_{n+m,0}.$$

Moreover, there exists a unique $(n+m)$–uple $(\hat\rho_1, \dots, \hat\rho_{n+m}) \in [0,1]^{n+m}$, such that

$$\hat\rho_i \in \begin{cases} \{\rho_{i,0}\} \cup (\tau(\rho_{i,0}), 1] & \text{if } 0 \le \rho_{i,0} \le \sigma, \\ [\sigma, 1] & \text{if } \sigma \le \rho_{i,0} \le 1, \end{cases} \quad i = 1, \dots, n, \tag{2.9}$$

and,

$$\hat\rho_j \in \begin{cases} [0, \sigma] & \text{if } 0 \le \rho_{j,0} \le \sigma, \\ \{\rho_{j,0}\} \cup [0, \tau(\rho_{j,0})) & \text{if } \sigma \le \rho_{j,0} \le 1, \end{cases} \quad j = n+1, \dots, n+m. \tag{2.10}$$

Fixed $i \in \{1, \dots, n\}$, if $\rho_{i,0} \le \hat\rho_i$ the solution is a shock:

$$\rho_i(x,t) = \begin{cases} \rho_{i0} & \text{if } x \le \frac{f(\hat\rho_i) - f(\rho_{i,0})}{\hat\rho_i - \rho_{i,0}} t, \\ \hat\rho_i & \text{otherwise}, \end{cases} \tag{2.11}$$

and if $\rho_{i,0} > \hat\rho_i$ the solution is a rarefaction:

$$\rho_i(x,t) = \begin{cases} \rho_{i0} & \text{if } x \le f'(\rho_{i,0}) t, \\ (f')^{-1}(\frac{x}{t}) & f'(\rho_{i0}) t \le x \le f'(\hat\rho_i) t, \\ \hat\rho_i & \text{if } x > f'(\hat\rho_i) t. \end{cases} \tag{2.12}$$

Proof Define the map

$$E : (\gamma_1, \dots, \gamma_n) \in \mathbb{R}^n \longmapsto \sum_{i=1}^{n} \gamma_i$$

and the sets

$$\Omega_i \doteq \begin{cases} [0, f(\rho_{i,0})], & \text{if } 0 \le \rho_{i,0} \le \sigma, \\ [0, f(\sigma)], & \text{if } \sigma \le \rho_{i,0} \le 1, \end{cases} \quad i = 1, \dots, n,$$

$$\Omega_j \doteq \begin{cases} [0, f(\sigma)], & \text{if } 0 \le \rho_{j,0} \le \sigma, \\ [0, f(\rho_{j,0})], & \text{if } \sigma \le \rho_{j,0} \le 1, \end{cases}$$

$$j = n+1, \dots, n+m,$$

$$\Omega \doteq \{(\gamma_1, \dots, \gamma_n) \in \Omega_1 \times \cdots \times \Omega_n \,|\, A \cdot (\gamma_1, \dots, \gamma_n)^T \in \Omega_{n+1} \times \cdots \times \Omega_{n+m}\}.$$

The set Ω is closed, convex and not empty. Furthermore, by (RP), ∇E is not orthogonal to any nontrivial subspace contained in a supporting hyperplane of Ω, therefore there exists a unique vector $(\hat\gamma_1, \dots, \hat\gamma_n) \in \Omega$ such that

$$E(\hat\gamma_1, \dots, \hat\gamma_n) = \max_{(\gamma_1, \dots, \gamma_n) \in \Omega} E(\gamma_1, \dots, \gamma_n).$$

For every $i \in \{1, \dots, n\}$, we choose $\hat\rho_i \in [0,1]$ such that

$$f(\hat\rho_i) = \hat\gamma_i, \quad \hat\rho_i \in \begin{cases} \{\rho_{i,0}\} \cup]\tau(\rho_{i,0}), 1], & \text{if } 0 \le \rho_{i,0} \le \sigma, \\ [\sigma, 1], & \text{if } \sigma \le \rho_{i,0} \le 1. \end{cases} \tag{2.13}$$

By $(\mathcal{F})$, $\hat\rho_i$ exists and is unique. Let

$$\hat\gamma_j \doteq \sum_{i=1}^{n} \alpha_{ji} \hat\gamma_i, \quad j = n+1, \dots, n+m,$$

and $\hat\rho_j \in [0,1]$ be such that

$$f(\hat\rho_j) = \hat\gamma_j, \quad \hat\rho_j \in \begin{cases} [0, \sigma], & \text{if } 0 \le \rho_{j,0} \le \sigma, \\ \{\rho_{j,0}\} \cup [0, \tau(\rho_{j,0})[, & \text{if } \sigma \le \rho_{j,0} \le 1. \end{cases} \tag{2.14}$$

Since $(\hat\gamma_1, \dots, \hat\gamma_n) \in \Omega$, $\hat\rho_j$ exists and is unique for every $j \in \{n+1, \dots, n+m\}$. The thesis is achieved. □

The solution on each road is given by the solution to Riemann problem with data $(\rho_{i0}, \hat\rho_i)$ for incoming roads and $(\hat\rho_j, \rho_{j0})$ for outgoing roads. Once the solution to Riemann problems is obtained, one can use a wave front tracking algorithm to build a sequence of approximate solutions.

Remark 2.7 In order to have admissible solutions to Riemann problems, we need that $(\rho_{i0}, \hat\rho_i)$ is solved by waves with negative speed, while $(\hat\rho_j, \rho_{j0})$ is solved by waves with positive speed. This is equivalent to conditions (2.9) and (2.10).

2.3 Existence of Solutions

Once the solution of Riemann problems at junctions is obtained, using that the speed of propagation is finite, one constructs solutions via wave-front tracking algorithm.

« ARCO 11831 layout: Large reference style: basic file: arco9004.tex (Aistes) aid: 9004 doctopic: OriginalPaper class: spr-twocol-v1 v.2007/05/18 Prn:19/05/2007; 13:34 p. 7»

Fig. 2 Traffic light

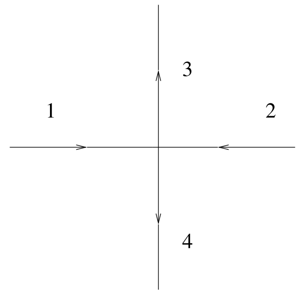

Now we are assuming to have junctions composed by two incoming and two outgoing roads. We are able to give an estimate of the total variation of the flux along an approximate wave front tracking solution.

Lemma 2.8 *Consider a road network $(\mathcal{I}, \mathcal{J})$. For some $K > 0$ we have the estimate on the flux variation*

$$\begin{aligned}\text{Tot.Var.}(f(\rho(t,\cdot))) &\le e^{Kt}\text{Tot.Var.}(f(\rho(0+,\cdot))) \\ &\le e^{Kt}\text{Tot.Var.}(f(\rho(0,\cdot))) + 2Rf(\sigma)\end{aligned}$$

for each $t \ge 0$, with R the total number of roads of the network.

Now we can state the existence result for the approximate solution.

Theorem 2.9 *Fix a road network $(\mathcal{I}, \mathcal{J})$. Given $C > 0$ and $T > 0$, there exists an admissible solution defined on $[0, T]$ for every initial data $\bar{\rho} \in \mathrm{cl}\{\rho : TV(\rho) \le C\}$, where cl is the closure in L^1_{loc}.*

For the proof of these results see again [9].

2.4 Examples

2.4.1 Traffic Light

In [8] the results on Cauchy problems have been extended to the case of time dependent coefficients α_{ij} with a finite number of discontinuities. Indeed, a possible assumption for the coefficients of junction with a traffic light is to take them as varying with red or green light.

At $t = 0$ the light-colour is fixed. On each incoming road, the effect of the traffic light can be qualitatively traced as follows. Equation (2.1) together with a boundary condition at $x = 0$ describes the evolution of the car densities. This boundary datum is defined as a piecewise constant periodic function of time whose period is $\Delta_g + \Delta_r$. When cars stop, a backward shock wave along the incoming road is created.

However, here we present a simpler modellization, that will be shown in Sect. 3.3.3. We consider a single road with a traffic light, where Δ_g and Δ_r are the two light phases: namely green and red. Traffic light is reproduced by the introduction of boundary conditions in the numerical approximation scheme in correspondence of the traffic light position along the road.

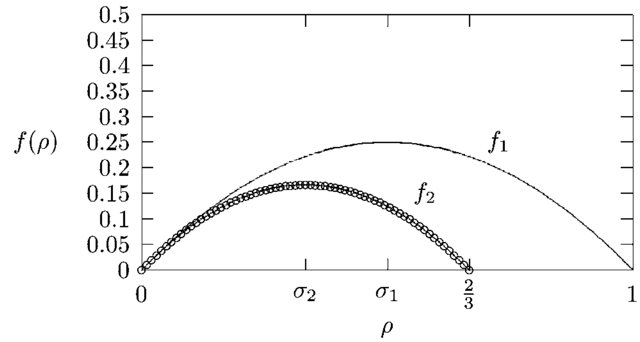

Fig. 3 The flux functions $f_1(\rho)$ and $f_2(\rho)$

Fig. 4 Interface at the bottleneck

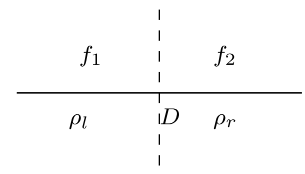

2.4.2 Bottleneck

The simplest application of the fluid-dynamic model presented in the previous section is represented by the bottleneck, which is a layout of the road characterized by a narrow passage that can constitute a point of congestion.

We consider two different flux functions along the road, where the conservation of cars is always expressed by (2.1) endowed with initial conditions $(\rho_{1,0}, \rho_{2,0})$ and boundary condition on the widest road $\rho_1(t, 0) = \rho_{1,b}(t)$. In the largest road the flux assumed is the following

$$f_1(\rho) = \rho(1-\rho), \quad \rho \in [0,1], \tag{2.15}$$

while, in the narrowest one, the flux considered is

$$f_2(\rho) = \rho\left(1 - \frac{3}{2}\rho\right), \quad \rho \in [0, 2/3]. \tag{2.16}$$

The maximum for the fluxes is unique:

$$f_1(\sigma_1) = \max_{[0,1]} f_1(\rho) = \frac{1}{4}, \quad \text{with } \sigma_1 = \frac{1}{2}, \tag{2.17}$$

$$f_2(\sigma_2) = \max_{[0,2/3]} f_2(\rho) = \frac{1}{6}, \quad \text{with } \sigma_2 = \frac{1}{3}. \tag{2.18}$$

A key role is played by the separation point between the two parts of the road, say D. Indicate by ρ_l the point placed on the left respect to D (that belongs to the widest part of

« ARCO 11831 layout: Large reference style: basic file: arco9004.tex (Aistes) aid: 9004 doctopic: OriginalPaper class: spr-twocol-v1 v.2007/05/18 Prn:19/05/2007; 13:34 p. 8»

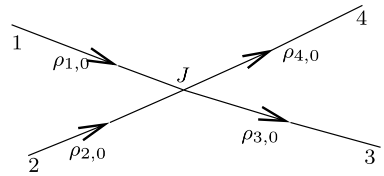

Fig. 5 A junction with two incoming and two outgoing roads

the street) and by ρ_r the point of the narrowest part on the right respect to S so that we can consider the bottleneck as composed by two roads. The maximization of f_1 and f_2 is performed following the rules, respectively

$$f_1^{\max}(\rho)=\begin{cases} f_1(\rho_l) & \text{if } \rho_l \le \sigma_1,\\ f_1(\sigma_1) & \text{if } \rho_l \ge \sigma_1,\end{cases}$$

$$f_2^{\max}(u)=\begin{cases} f_2(\sigma_2) & \text{if } \rho_r \le \sigma_2,\\ f_2(\rho_r) & \text{if } \rho_r \ge \sigma_2\end{cases}$$

and the intersection point between the two intervals is obtained taking the minimum

$$\gamma=\min\{f_1^{\max}(\rho_l), f_2^{\max}(\rho_r)\}, \tag{2.19}$$

with ρ_l and ρ_r instantaneously fixed.

As the maximum density allowed in the second part is given by $\sigma_2=\frac{1}{6}$, the creation of queues occurs when the density on the first road verifies

$$\rho(1-\rho)=\frac{1}{6} \Longleftrightarrow \bar\rho=\frac{1-\sqrt{\frac{1}{3}}}{2}\simeq 0.21. \tag{2.20}$$

Hence, if we start from an empty configuration (namely $\rho_{1,0}=1, \rho_{2,0}=0$) and the boundary datum satisfies the condition $\rho_{1,b}(t)<\bar\rho$, then there is no formation of shocks propagating backwards.

2.4.3 *Two Incoming and Two Outgoing Roads*

Here we consider the particular case of a junction with two outgoing and two incoming roads. The flux function is taken as follows:

$$f(\rho)=\rho(1-\rho).$$

The incoming roads are indicated as 1 and 2, while the outgoing roads are 3 and 4. In order to determine the region for the maximization of the flux, we impose a restriction on the initial data. For roads $i=1,2$ the maximum flux reads:

$$f_i^{\max}=\begin{cases} f(\sigma) & \text{if } \rho_{i,0}\in[\sigma,\rho_{\max}],\\ f(\rho_{i,0}) & \text{if } \rho_{i,0}\in[0,\sigma),\end{cases}$$

while for roads $j=3,4$ the maximum flux is:

$$f_j^{\max}=\begin{cases} f(\sigma) & \text{if } \rho_{j,0}\in[0,\sigma],\\ f(\rho_{j,0}) & \text{if } \rho_{j,0}\in(\sigma,\rho_{\max}].\end{cases}$$

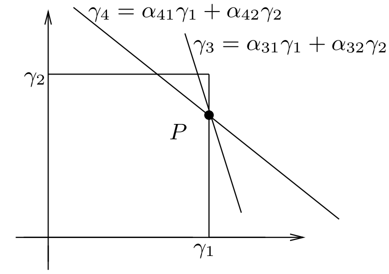

Fig. 6 Maximization region

Fig. 7 A junction with two incoming and one outgoing roads

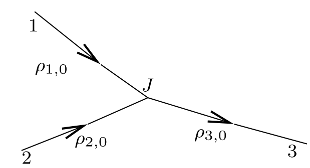

We obtain the two sets:

$$\Omega_{12}=[0,f(\bar\rho_{10})]\times[0,f(\bar\rho_{20})] \quad \text{and}$$
$$\Omega_{34}=[0,f(\bar\rho_{30})]\times[0,f(\bar\rho_{40})]$$

and maximize the sum of fluxes on the region $\Omega_{12}\cap A^{-1}(\Omega_{34})$.

Introducing the notation $\gamma_l=f(\bar\rho_{l,0})$, $l=1,2,3,4$, we have

$$\max(\gamma_1+\gamma_2)=\hat\gamma_1+\hat\gamma_2$$

and we obtain $\hat\gamma_3$ and $\hat\gamma_4$, through the following relation

$$A\begin{pmatrix}\hat\gamma_1\\ \hat\gamma_2\end{pmatrix}=\begin{pmatrix}\hat\gamma_3\\ \hat\gamma_4\end{pmatrix}\in\Omega_{34}, \tag{2.21}$$

where the traffic distribution matrix reads

$$A=\begin{pmatrix}\alpha_{31} & \alpha_{32}\\ \alpha_{41} & \alpha_{42}\end{pmatrix}. \tag{2.22}$$

The solution is:

$$(\hat\gamma_1,\hat\gamma_2,\hat\gamma_3,\hat\gamma_4)$$

and the corresponding $\hat\rho_l$ are given by

$$f(\hat\rho_l)=\hat\gamma_l, \quad l=1,\dots,4. \tag{2.23}$$

In particular, we invert (2.23) using the following rules:

$$i=1,2, \quad \hat\rho_i\in\begin{cases}\{\rho_{i,0}\}\cup]\tau(\rho_{i,0}),1], & \text{if } 0\le\rho_{i,0}\le\sigma,\\ [\sigma,1], & \text{if } \sigma\le\rho_{i,0}\le 1,\end{cases} \tag{2.24}$$

$$j=3,4, \quad \hat\rho_j\in\begin{cases}[0,\sigma], & \text{if } 0\le\rho_{j,0}\le\sigma,\\ \{\rho_{j,0}\}\cup[0,\tau(\rho_{j,0})[, & \text{if } \sigma\le\rho_{j,0}\le 1.\end{cases} \tag{2.25}$$

« ARCO 11831 layout: Large reference style: basic file: arco9004.tex (Aistes) aid: 9004 doctopic: OriginalPaper class: spr-twocol-v1 v.2007/05/18 Prn:19/05/2007; 13:34 p. 9»

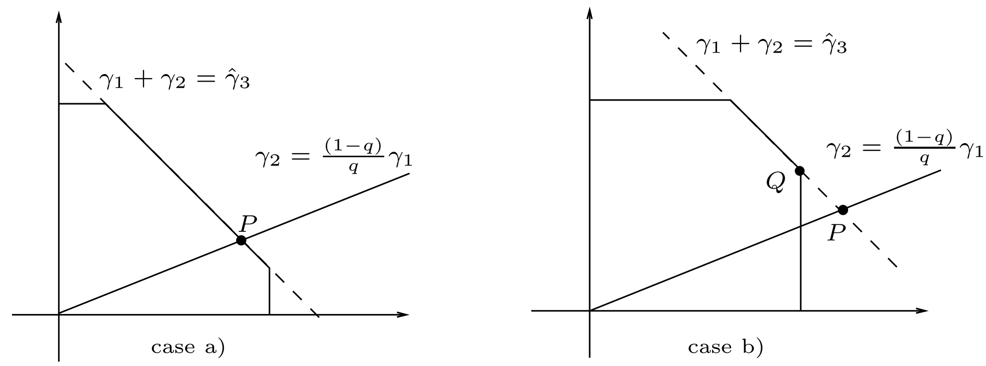

Fig. 8 Solutions to Riemann problem for rule (C)

2.4.4 *Two Incoming and One Outgoing Roads*

In order to show how rule (C) previously introduced works, let us consider a junction with one outgoing and two incoming roads. As explained in Sect. 2, condition (RP) on A cannot hold for crossings with two incoming and one outgoing roads. Then we introduce a further parameter, namely q, with the following meaning: when the number of cars is too big to let all of them go through crossing, there is a yielding rule that describes the percentage of cars going through the crossing, that comes from the first road. Let us fix a crossing with two incoming roads $[a_i, b_i]$, $i = 1, 2$, and one outgoing road $[a_3, b_3]$ and assume that a right of way parameter $q \in]0, 1[$ is given. The solution to the Riemann problem with initial data $(\rho_{1,0}, \rho_{2,0}, \rho_{3,0})$ is composed by a single wave on each road connecting the initial states to $(\hat{\rho}_1, \hat{\rho}_2, \hat{\rho}_3)$ determined as follows (cfr. with the solution to the Riemann problem in the two incoming-two outgoing roads). Define $\gamma_i^{\max}$, $i = 1, 2$ and $\gamma_3^{\max}$ in the following way:

$$\gamma_i^{\max} = \begin{cases} f(\rho_{i,0}) & \text{if } \rho_{i,0} \in [0, \sigma], \\ f(\sigma) & \text{if } \rho_{i,0} \in]\sigma, 1], \end{cases}$$

and

$$\gamma_3^{\max} = \begin{cases} f(\sigma) & \text{if } \rho_{3,0} \in [0, \sigma], \\ f(\rho_{3,0}) & \text{if } \rho_{3,0} \in]\sigma, 1]. \end{cases}$$

The quantities $\gamma_i^{\max}$ represent the maximum flux that can be reached by a single wave solution on each road. Since our goal is to maximize going through traffic, we set:

$$\hat{\gamma}_3 = \min\{\gamma_1^{\max} + \gamma_2^{\max}, \gamma_3^{\max}\}. \tag{2.26}$$

Consider the space (γ_1, γ_2), then rule (C) is respected by points on the line:

$$\gamma_2 = \frac{1-q}{q}\gamma_1. \tag{2.27}$$

Thus define P to be the point of intersection of the line (2.27) with the line $\gamma_1 + \gamma_2 = \hat{\gamma}_3$. Recall that the final fluxes should belong to the region:

$$\Omega = \{(\gamma_1, \gamma_2) : 0 \le \gamma_i \le \gamma_i^{\max}\},$$

then we distinguish two cases:

(a) P is inside Ω,
(b) P is outside Ω.

In the first case we set $(\hat{\gamma}_1, \hat{\gamma}_2) = P$, while in the second we set $(\hat{\gamma}_1, \hat{\gamma}_2) = Q$, where Q is the point of the segment $\Omega \cap \{(\gamma_1, \gamma_2) : \gamma_1 + \gamma_2 = \hat{\gamma}_3\}$ closest to the line (2.27). We show in Fig. 8 the cases (a)–(b).

Then we determine $\hat{\rho}_i$ with rules (2.13) and (2.14) presented in the previous section.

2.5 Traffic Circles

Here we deal with the following traffic regulation problem: given a junction with some incoming roads and some outgoing ones, is it preferable to regulate the flux via a traffic light or via a traffic circle on which the incoming traffic enters continuously? More precisely, assuming that drivers arriving at the junction distribute on the outgoing roads according to some known coefficients, our purpose is to understand which solution performs better from the point of view of total amount of cars going through the junction.

In order to treat this problem we need a model that describes the above situation and provides an accurate analysis. To this aim we consider the fluid dynamic model based on (2.1), proposed in [9] and adapted in a suitable way in order to treat the case of traffic circles in [8], where a traffic circle can be modelled using rule (C). Consider a general network, as the traffic circle, with junctions having either one incoming and two outgoing or two incoming and one outgoing roads. Therefore at each junction we can refer to the cases represented in Sects. 2.4.3, 2.4.4. Once the solution to Riemann problems is fixed then we can introduce the definition of admissible solutions as in [8]. Similarly we can

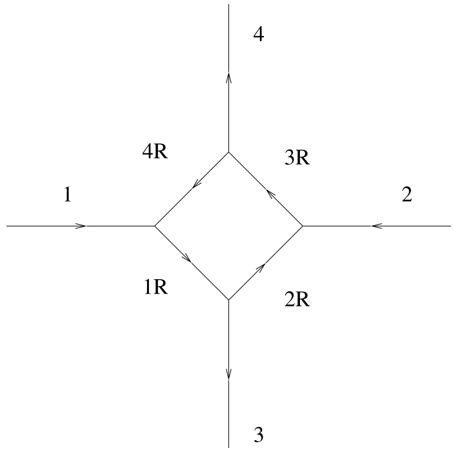

Fig. 9 Traffic circle

deal with the case of coefficients α_{ij} and right of way parameters q_k depending on time.

Notice that we only treat the case of the single-lane traffic circles. A model for the multi-lane traffic circles is proposed in [8].

Consider a simple network representing a traffic circle composed by four roads, named $1, \dots, 4$, the first two incoming in the circle and the other two outgoing. In addition there are four roads $1R, \dots, 4R$ that form the circle as in Fig. 9. As before the parametrization of roads is given by $[a_i, b_i]$, $i = 1, \dots, 4$, and $[a_{iR}, b_{iR}]$, $i = 1, \dots, 4$. We assign a traffic distribution matrix A describing how traffic coming from roads 1, 2 distributes through roads 3 and 4, passing by the intermediate roads of the circle. Two parameters are fixed, namely $\alpha, \beta \in]0, 1[$, such that

(C1) If M cars reach the circle from road 1, then αM drive to road 3 and $(1-\alpha)M$ drive to road 4,
(C2) If M cars reach the circle from road 2, then βM drive to road 4 and $(1-\beta)M$ drive to road 3.

Then we can determine the distribution coefficients, see [8].

3 Numerical Approximation

In order to find approximate solutions, we adapt to the problem the classical Godunov scheme (FG) and the 3-Velocities Kinetic scheme of first and second order (K3V), already presented and discussed in [7]. Concerning the discrete kinetic scheme, we recall that is a quite recent scheme for conservation laws [1, 21], applied to traffic flow problem in [7]. The kinetic scheme we consider are known for the Cauchy problem. They were first introduced in the framework of the Boltzmann approach of hydrodynamic problems, see [11, 22, 23]. A kinetic interpretation of flux splitting schemes is given in the paper by A. Harten, P.D. Lax,

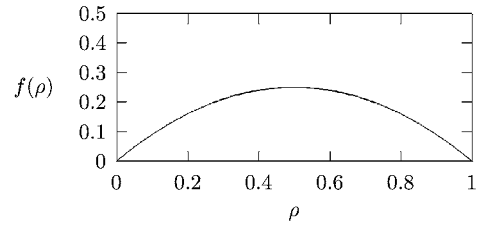

Fig. 10 The flux function

and B. van Leer [15]. For general conservation laws, S. Jin and Z. Xin introduced a relaxation approximation and constructed related numerical schemes, which are equivalent to kinetic schemes with discrete velocities, for the Cauchy problem [17]. A quite complete investigation on second order relaxation and discrete kinetic schemes for general systems of conservation laws in several space variables and with boundary conditions was developed in [1] and [2]. The interactions at junctions are solved by the use of a Linear Programming algorithm that computes the maximized fluxes for all the schemes.

For definitiveness, we choose the following flux

$$f(\rho) = v_{\max}\rho\left(1 - \frac{\rho}{\rho_{\max}}\right), \tag{3.1}$$

and, setting for simplicity $\rho_{\max} = 1 = v_{\max}$:

$$f(\rho) = \rho(1-\rho). \tag{3.2}$$

The maximum $\sigma = \frac{1}{2}$ is unique: $f(\sigma) = \max_{[0,1]} f(\rho) = f^{\max} = \frac{1}{4}$.

Remark 3.1 However, any concave flux could be assumed instead of (3.1).

The graph in Fig. 10 represents the flux function $f(\rho)$.

We define a *numerical grid* in $(0, T) \times \mathbb{R}^L$ using the following notations:

- Δx is the space grid size;
- Δt is the time grid size;
- $(t_h, x_m) = (h\Delta t, m\Delta x)$ for $h \in \mathbb{N}$ and $m \in \mathbb{Z}$ are the grid points.

For a function v defined on the grid we write $v_m^h = v(t_h, x_m)$ for m, h varying on a subset of $\mathbb{Z}$ and $\mathbb{N}$ respectively. We also use the notation u_m^h for $u(t_h, x_m)$ when u is a continuous function on the (t, x) plane.

3.1 Godunov Scheme [12, 13]

A good numerical method to solve the equations along roads is represented by the Godunov scheme, which is based on exact solutions to Riemann problems, [12, 13]. This method was introduced in 1959 as an approach to solving the Euler equations of gas dynamics in the presence of shock waves, for details see for instance [12]. The idea is the following: first the initial datum is approximated by a piecewise constant function; then the corresponding Riemann problems are solved exactly and a global solution is simply obtained by piecing them together; finally, one takes the mean and proceeds by induction.

Let us now detail the scheme. We take a piecewise constant approximation of the initial datum:

$$v_m^0 = \frac{1}{\Delta x}\int_{x_{m-1/2}}^{x_{m+1/2}} u_0(x)dx, \quad m \geq 0 \tag{3.3}$$

and the scheme defines v_m^h recursively starting from v_m^0. Waves in two neighbour cells do not interact before time Δt if the CFL condition holds:

$$\Delta t \sup_{m,h}\Big\{\sup_{u\in I(u^h_{m-1/2},u^h_{m+1/2})} |f'(u)|\Big\} \leq \frac{1}{2}\Delta x. \tag{3.4}$$

Solutions to Riemann problems from $x_{m-1/2}$ are taken and then projected on a piecewise constant function by

$$v_m^{h+1} = \frac{1}{\Delta x}\int_{x_{m-1/2}}^{x_{m+1/2}} v^{\Delta}(t_{h+1}, x)dx. \tag{3.5}$$

Since v is an exact solution of (2.1), we can use the Gauss-Green formula in (2.1) to compute v^{h+1}.

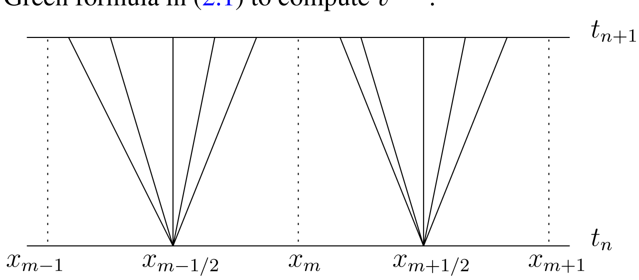

Under the CFL condition

$$\Delta t \sup_{m,h}\Big\{\sup_{u\in I(u^h_{m-1/2},u^h_{m+1/2})} |f'(u)|\Big\} \leq \Delta x, \tag{3.6}$$

the waves, generated by Riemann solutions, do not influence the solution in $x = x_{m+1/2}$, for $t \in (t_h, t_{h+1})$. As the flux is time invariant and continuous, we can put it out of the integral and, setting $g^G(u,v) = F(W_R(0; u, v))$, with $W_R(\frac{x}{t}; v_-, v_+)$ the self-similar solution between v_- and v_+, and, under the condition (3.6), the scheme can be written as:

$$v_m^{h+1} = v_m^h - \frac{\Delta t}{\Delta x}\big(g^G(v_m^h, v_{m+1}^h) - g^G(v_{m-1}^h, v_m^h)\big). \tag{3.7}$$

Then we define the projection of the exact solution on a piecewise constant function

$$v_m^{h+1} = \frac{1}{\Delta x}\int_{x_m}^{x_{m+1}} v^{\Delta}(x, t_{h+1})dx. \tag{3.8}$$

Since v is an exact solution of (2.1), we use the Gauss-Green formula in (2.1) to compute this value. Under the CFL condition, the solutions are locally given by the Riemann problems and in particular the flux in $x = x_{m+1/2}$ for $t \in (t_h, t_{h+1})$ is given by

$$f(u(t, x_{m+1/2})) = f(W_R(0; v_{m-1}^k, v_m^k)),$$

where $W_R(\frac{x}{t}; v_-, v_+)$ is the self-similar solution between v_- and v_+. As the flux is time invariant and continuous, we can put it out of the integral and, setting $g^G(u,v) = f(W_R(0; u, v))$ under the condition (3.4), the scheme can be written as:

$$v_m^{h+1} = v_m^h - \frac{\Delta t}{\Delta x}\big(g^G(v_m^h, v_{m+1}^h) - g^G(v_{m-1}^h, v_m^h)\big). \tag{3.9}$$

The numerical flux g^G, for the flux we are considering, has the expression:

$$g^G(u,v) = \begin{cases} \min(f(u), f(v)) & \text{if } u \leq v\,, \\ f(u) & \text{if } v < u < \sigma, \\ f^{\max} & \text{if } v < \sigma < u, \\ f(v) & \text{if } \sigma < v < u. \end{cases}$$

3.2 Kinetic Method for a Boundary Value Problem [1, 2]

Here we present the kinetic scheme for initial-boundary value conservation equations:

$$u_t + F(u)_x = 0, \tag{3.10}$$

$$u(0, x) = u_0(x), \quad x \geq 0, \tag{3.11}$$

$$u(t, 0) = u_b(t), \quad t \geq 0, \tag{3.12}$$

and (3.12) can be imposed only where it is compatible with the trace of the solution to the problem and with the flux F. We have $u(t,x) \in \mathbb{R}$ for $t \geq 0$, $x \geq 0$, and F is a Lipschitz continuous function.

A kinetic approximation of the problem (3.10–3.12) is obtained solving the following BGK-like system of K nonlinear equations:

$$\partial_t f_k^\varepsilon + \lambda_k \partial_x f_k^\varepsilon = \frac{1}{\varepsilon}\big(M_k(u^\varepsilon) - f_k^\varepsilon\big), \quad k = 1, \ldots, K, \tag{3.13}$$

where the λ_k are fixed velocities (a set of real numbers not all zero), ϵ is a positive parameter, and each f_k^ϵ is a function of $\mathbb{R}^+ \times [0,T] \times \mathbb{R}^+$ with values in $\mathbb{R}$. We impose the corresponding initial and boundary data:

$$f_k^\epsilon(0, x) = M_k(u_0(x)), \quad x \in \mathbb{R}^+, \tag{3.14}$$

$$f_k^\epsilon(t, 0) = M_k(u_b(t)) \quad \forall \lambda_k > 0 \text{ and } t \geq 0. \tag{3.15}$$

Functions M_k, $k = 1, \ldots, N$, are the Maxwellian functions depending on u^ϵ, F and λ_k. To have the convergence of $u^\varepsilon =$

« ARCO 11831 layout: Large reference style: basic file: arco9004.tex (Aistes) aid: 9004 doctopic: OriginalPaper class: spr-twocol-v1 v.2007/05/18 Prn:19/05/2007; 13:34 p. 12»

$\sum_{k=1}^N f_k^\varepsilon$ when $\varepsilon \to 0$ towards the solution of the problem (3.10–3.12), we need to impose the following compatibility conditions:

$$\sum_{k=1}^N M_k(u) = u, \qquad \sum_{k=1}^N \lambda_k M_k(u) = F(u), \tag{3.16}$$

that show the link between problem (3.10) and system (3.13).

A sufficient condition for convergence is that M is Monotone Non Decreasing on I, [21]. Then the following subcharacteristic condition is satisfied for all $u \in I$:

$$\min_k \lambda_k \le F'(u) \le \max_k \lambda_k. \tag{3.17}$$

3.2.1 Kinetic Approximations

Here follows a presentation of the different approximations we used in kinetic schemes already proposed in [21].

- *Two velocities model.* $K = 2$, $\lambda_1 = -\lambda_2 = -\lambda$. We approximate the scalar conservation law (2.1) by a relaxation system which is diagonalized in the form

  $$\begin{cases} \partial_t f_1^\varepsilon - \lambda \partial_x f_1^\varepsilon = \frac{1}{\varepsilon}(M_1(u^\varepsilon) - f_1^\varepsilon) \\ \partial_t f_2^\varepsilon + \lambda \partial_x f_2^\varepsilon = \frac{1}{\varepsilon}(M_2(u^\varepsilon) - f_2^\varepsilon). \end{cases}$$

  The associated Maxwellian functions are

  $$M_1(u) = \frac{1}{2}\left(u - \frac{F(u)}{\lambda}\right), \qquad M_2(u) = \frac{1}{2}\left(u + \frac{F(u)}{\lambda}\right).$$

  In order to respect the monotonicity condition MND on $I \subset \mathbb{R}$, we have the following relation for the velocity vector λ:

  $$\max_{u \in I} |F'(u)| < \lambda. \tag{3.18}$$

- *Three velocities model.* Dealing with more velocities corresponds to more accurate approximation schemes. Take $K = 3$ and the velocities $\lambda_3 = -\lambda_1 = \lambda > 0$, $\lambda_2 = 0$. The approximate kinetic system has the Maxwellian functions given by

  $$M_1(u) = \frac{1}{\lambda}\begin{cases} 0, & \text{if } u \le \frac{1}{2}, \\ u(u-1) + \frac{1}{4}, & \text{if } u \ge \frac{1}{2}, \end{cases}$$

  $$M_2(u) = \begin{cases} (1 - \frac{1}{\lambda})u + \frac{1}{\lambda}u^2, & \text{if } u \le \frac{1}{2}, \\ (1 + \frac{1}{\lambda})u - \frac{1}{\lambda}u^2 - \frac{1}{2\lambda}, & \text{if } u \ge \frac{1}{2}, \end{cases}$$

  $$M_3(u) = \frac{1}{\lambda}\begin{cases} u(1-u), & \text{if u} \le \frac{1}{2}, \\ \frac{1}{4}, & \text{if } u \ge \frac{1}{2}. \end{cases}$$

  At the boundary we impose $f_3(t,0) = M_3(u_b(t))$ and the Maxwellian are MND if and only if the condition (3.18) is satisfied. In this case (3.18) reads

  $$0 \le M_2'(u) \le 1 - \frac{|F'(u)|}{\lambda}.$$

  This model, at first order, is the kinetic expression of the Engquist-Osher scheme.

3.2.2 Numerical Scheme

Following [1, 2], we discretize the problem (3.13–3.15) and making ϵ tend to zero, we obtain a numerical scheme for the initial boundary value problem for the conservation law (3.10), see [1] for more details and convergence results. Here we consider the three velocities model. As usual, we discretize data of the problem by a piecewise constant approximation:

$$f_{-1,k}^h = M_k(u_b^h), \quad k = 1, \dots, K,\ h = 0, \dots, M-1,$$
$$f_{m,k}^0 = M_k(u_m^0), \quad m \in \mathbb{N}.$$

The operators used to solve system (3.13) are splitted into the *transport* part and the *collision* part.

For the transport contribute, the scheme written in the Harten formulation including both first and second order in space approximation reads:

$$m \ge 0, \quad \begin{cases} f_{m,k}^{h+\frac{1}{2}} = f_{m,k}^h(1 - D_{m-\frac{1}{2},k}^h) + D_{m-\frac{1}{2},k}^h f_{m-1,k}^h, \\ \quad \text{if } \lambda_k > 0, \\ f_{m,k}^{h+\frac{1}{2}} = f_{m,k}^h(1 - D_{m+\frac{1}{2},k}^h) + D_{m+\frac{1}{2},k}^h f_{m+1,k}^h, \\ \quad \text{if } \lambda_k \le 0. \end{cases} \tag{3.19}$$

Note that it is necessary to assign the boundary value $f_{b,k}^h = f_{-1,k}^h$ only for positive velocities. A first order in space upwind approximation is chosen:

$$D_{m-\frac{1}{2},k}^h = D_{m+\frac{1}{2},k}^h = \xi_k = |\lambda_k|\frac{\Delta t}{\Delta x}$$

and in that case (3.19) is well defined even for $m = 0$.

The transport part can be approximated by a second order scheme as follows. Starting from $f_{m,k}^h$ we build a piecewise linear function:

$$\tilde{f}_{m,k}^h(x) = f_{m,k}^h + (x - x_m)\sigma_{m,k}^h, \quad x \in (x_{m-\frac{1}{2}}, x_{m+\frac{1}{2}}),$$

where $\sigma_{m,k}^h$ are limited slopes and we solve exactly the transport equations on $[t_h, t_{n+1}]$. Projecting the solution on the set of piecewise constant functions on the cells, we obtain the explicit expression for $D_{m+\frac{1}{2},k}^h$:

$$D_{m+\frac{1}{2},k}^h = \xi_k\left(1 + \operatorname{sgn}(\lambda_k)\Delta x \frac{(1-\xi_k)}{2}\frac{(\sigma_{m+1,k}^h - \sigma_{m,k}^h)}{\Delta f_{m+\frac{1}{2},k}^h}\right), \tag{3.20}$$

with the convention that if $\Delta f^h_{m+\frac{1}{2},k}=0$, then $D^h_{m+\frac{1}{2},k}=\xi_k=|\lambda_k|\frac{\Delta t}{\Delta x}$. Note that if $\lambda_k>0$ (3.20) is defined for $m\geq -1$, in the other cases is available for $m\geq 0$. The slopes $\sigma^h_{m,k}$ for $m\geq 1$ are:

$$\sigma^h_{m,k}=\operatorname{minmod}\left(\frac{\Delta f^h_{m+\frac{1}{2},k}}{\Delta x},\frac{\Delta f^h_{m-\frac{1}{2},k}}{\Delta x}\right),$$

with $\Delta f^h_{m+\frac{1}{2},k}=f^h_{m+1,k}-f^h_{m,k}$ and $\operatorname{minmod}(a,b)=\min(|a|,|b|)\frac{\operatorname{sgn}(a)+\operatorname{sgn}(b)}{2}$. For the convergence results see [1]. The time step restriction for both cases is

$$\max_{1\leq k\leq K}|\lambda_k|\Delta t\leq\Delta x. \tag{3.21}$$

Then we use the solution obtained from the previous scheme as the initial condition for collision system. Under the compatibility conditions (3.16) we find the exact solution of the system, that for $\epsilon\to 0$ is

$$f^{h+1}_{m,k}=M_k(u_m^{h+\frac{1}{2}})=M_k(u_m^{h+1}),\quad m\geq 0,\ n\geq 1 \tag{3.22}$$

and the identity holds

$$u_m^{h+1}=\sum_k f^{h+\frac{1}{2}}_{m,k}=u_m^{h+\frac{1}{2}}. \tag{3.23}$$

Assuming that the Maxwellian functions are MND, we have the usual CFL condition

$$\max_u|F'(u)|\Delta t\leq\Delta x$$

and, from the transport part of the scheme, we have to impose the time step restriction in (3.21).

3.3 Boundary Conditions and Conditions at Junctions

Here we impose boundary conditions for roads with one of the endpoints not connected to any junction: in that case we impose at the boundary the given boundary datum or a Neumann condition (only for outgoing roads).

We also assign boundary conditions for roads with endpoints connected to junctions: we impose at the boundary the boundary datum determined by interactions which is computed by a simplex-type linear programming algorithm.

3.3.1 Godunov Scheme

Boundary Conditions Suppose to assign a condition at the incoming boundary $x=0$:

$$u(t,0)=\rho_b^{\text{inc}}(t),\quad t>0$$

and study equation only for $x>0$. Now we are considering the initial-boundary value problem (3.10–3.11–3.12) with $u_0\in C^1(\mathbb{R}^+)$, $u_b(t)\in C^1((0,T))$, $F\in C^1(\mathbb{R})$. It is not easy to find a function u that satisfies (3.12) in a classical sense, because, in general, the boundary data cannot be assumed. One seeks a condition which is to be effective only in the inflow part of the boundary. Following [4] the rigorous way of assigning the boundary condition is:

$$\max_{k\in I(u(t,0),\rho_b^{\text{inc}}(t))}\left\{\operatorname{sgn}(u(t,0)-\rho_b^{\text{inc}}(t))[F(u(t,0))-F(k)]\right\}=0. \tag{3.24}$$

We practically proceed by inserting a ghost cell and defining

$$v_0^{h+1}=v_0^h-\frac{\Delta t}{\Delta x}\left(g^G(v_0^h,v_1^h)-g^G(u^h_{(\text{inc})},v_0^h)\right), \tag{3.25}$$

where

$$u^h_{(\text{inc})}=\frac{1}{\Delta t}\int_{t_h}^{t_{h+1}}\rho_b^{\text{inc}}(t)dt$$

takes the place of v^h_{-1}.

An outgoing boundary can be treated analogously. Let $x<x_L$. Then the discretization reads:

$$v_L^{h+1}=v_L^h-\frac{\Delta t}{\Delta x}\left(g^G(v_L^h,u^h_{(\text{out})})-g^G(v^h_{L-1},v^h_L)\right), \tag{3.26}$$

where

$$u^h_{(\text{out})}=\frac{1}{\Delta t}\int_{t_h}^{t_{h+1}}\rho_b^{\text{out}}(t)dt$$

takes the place of v^h_{L+1}, that is a ghost cell value.

Conditions at a Junction For roads connected to a junction at the right endpoint we set

$$v_L^{h+1}=v_L^h-\frac{\Delta t}{\Delta x}\left(\hat{\gamma}_i-g^G(v^h_{L-1},v^h_L)\right),$$

while for roads connected to a junction at the right endpoint we have

$$v_0^{h+1}=v_0^h-\frac{\Delta t}{\Delta x}\left(g^G(v_0^h,v_1^h)-\hat{\gamma}_j\right),$$

where $\hat{\gamma}_i,\hat{\gamma}_j$ are the maximized fluxes described in Sect. 2.

Remark 3.2 For Godunov scheme there is no need to invert the flux f to put it in the scheme, as the Godunov flux coincides with the Riemann flux. In this case it suffices to insert the computed maximized fluxes directly in the scheme.

3.3.2 Kinetic Schemes

Boundary Conditions For $m=0$ we take for the boundary

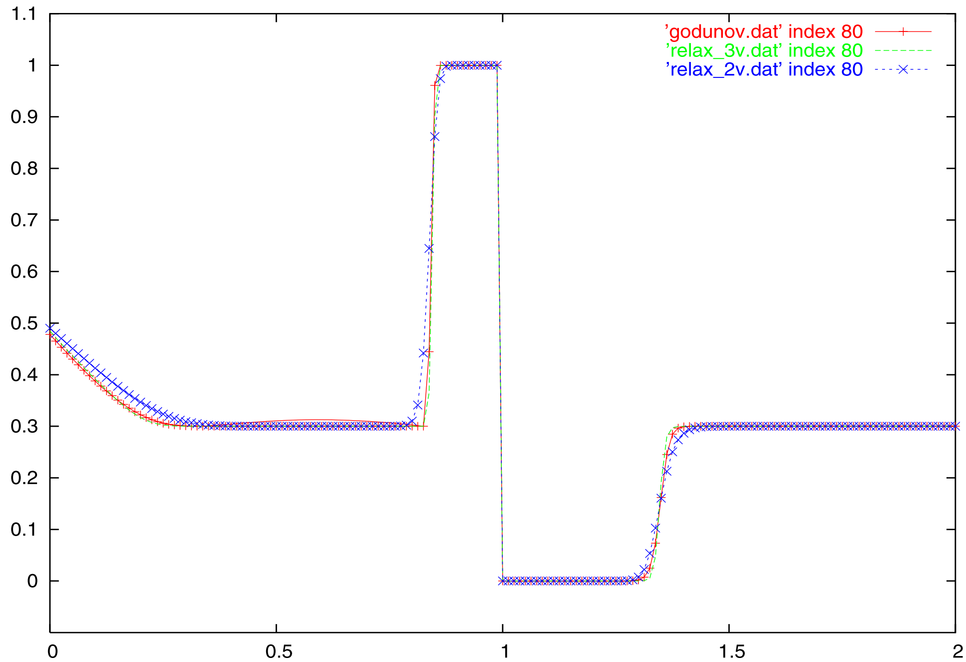

Fig. 11 Density when the light is red, $h = 0.0125$, $T = 0.5$

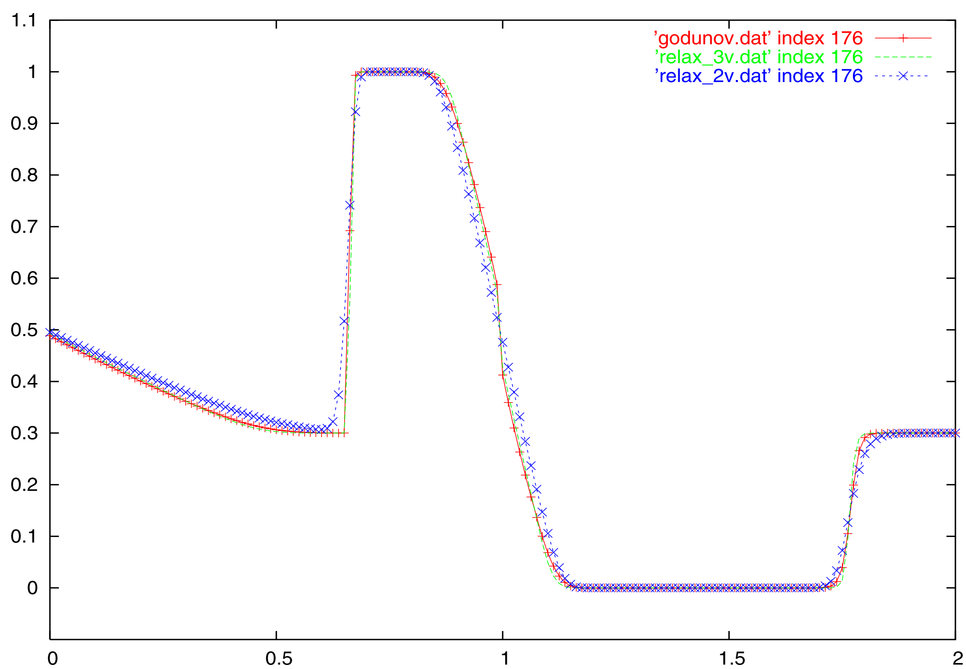

Fig. 12 Density after the light turns green, $h = 0.0125$, $T = 1.1$

$\sigma^h_{-1,k} = 0.$

In this case, the slope $\sigma^h_{0,k}$ can be defined as

- For $\lambda_k > 0$:

$$\sigma^h_{0,k} = \operatorname{minmod}\left(\frac{f^h_{1,k} - f^h_{0,k}}{\Delta x}, 2\frac{f^h_{0,k} - M_k(u^h_b)}{\Delta x}\right),$$

where u^h_b is the boundary condition;

- For $\lambda_k < 0$:

$$\sigma^h_{0,k} = \frac{f^h_{1,k} - f^h_{0,k}}{\Delta x}.$$

When $m = L$ the scheme for $\lambda_k < 0$ requires the values $f^h_{L+1,k}, f^h_{L+2,k}$, that can be obtained, for instance, by imposing a Neumann condition.

« ARCO 11831 layout: Large reference style: basic file: arco9004.tex (Aistes) aid: 9004 doctopic: OriginalPaper class: spr-twocol-v1 v.2007/05/18 Prn:19/05/2007; 13:34 p. 15»

Fig. 13 The light is again red, high density at $x = 1$, $h = 0.0125$, $T = 2.0$

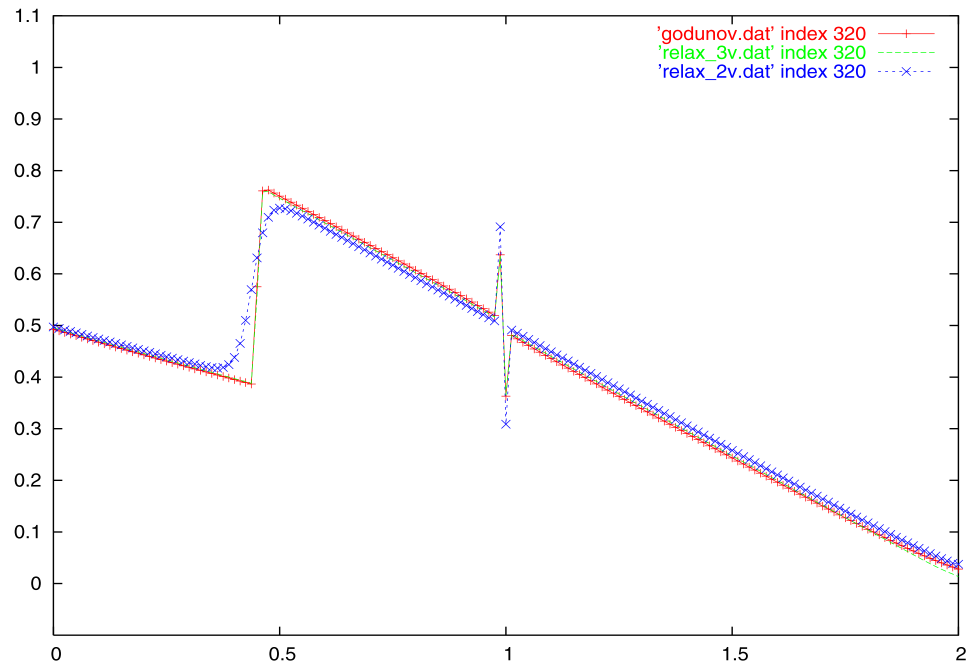

Fig. 14 High density at the entrance ($x = 0$), $\Delta_g = \Delta_r = 1.0$, $h = 0.0125$, $T = 3.8$

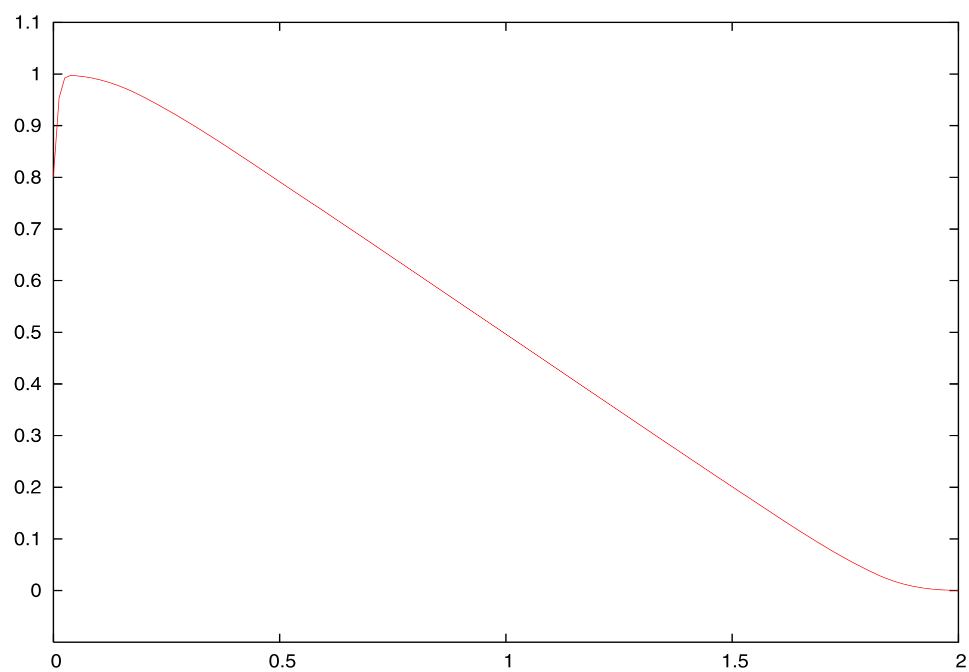

Conditions at a Junction As usual, in order to impose the boundary condition at a junction we need to examine the links between the roads. At the right boundary ($m = L$) of roads linked to the junction on the right endpoint one has:

$$f_{L,k}^{h+\frac{1}{2}} = f_{L,k}^{h}(1 - D_{L+\frac{1}{2},k}^{h}) + D_{L+\frac{1}{2},k}^{h} f_{L+1,k}^{h}, \quad \text{for } \lambda_k < 0,$$

with

$$f_{L+1,k}^{h} = M_k(f^{-1}(\hat{\gamma}_i)).$$

Moreover we use the Neumann condition $f_{L+2,k}^{h} = f_{L+1,k}^{h}$ for roads which are not linked to the junction on the right. At the left boundary ($m = 0$) of roads linked to the junction on the left endpoint the scheme in case $\lambda_k > 0$ reads:

$$f_{0,k}^{h+\frac{1}{2}} = f_{0,k}^{h}(1 - D_{-\frac{1}{2},k}^{h}) + D_{-\frac{1}{2},k}^{h} f_{-1,k}^{h},$$

with

$$f_{-1,k}^{h} = M_k(f^{-1}(\hat{\gamma}_j)).$$

Table 1 Convergence order γ, defined in (4.1), and errors of the approximation schemes Godunov (G), 3 velocities Kinetic methods of first order ($3VK_1$) and of second order ($3VK_2$) for data 4.5, $\Delta_g = \Delta_r = 1.0$, $T = 2$

	G		$3VK_1$		$3VK_2$	
h	γ	L^1 Error	γ	L^1 Error	γ	L^1 Error
0.1	1.074739	0.048958	1.098426	0.050723	1.518485	0.026815
0.05	0.717578	0.023243	0.740926	0.023689	1.584962	0.009360
0.025	0.732966	0.014135	0.738094	0.014174	1.608739	0.003120
0.0125	0.743919	0.008504	0.741168	0.008498	1.584962	0.001057
0.00625	0.779725	0.005078	0.764019	0.005084	1.560714	0.000341
0.003125	0.840073	0.002958	0.829557	0.002994	1.580145	0.000114

Table 2 Orders and errors of the approximation schemes Godunov (G), Kinetic of first order ($3VK_1$) and of second order ($3VK_2$) for data (4.6), $T = 0.5$

	G		$3VK_1$		$3VK_2$	
h	γ	L^1 Error	γ	L^1 Error	γ	L^1 Error
0.1	1.51554	$3.347e-002$	1.14981	$2.886e-002$	1.19519	$2.931e-002$
0.05	0.89752	$1.170e-002$	0.83645	$1.301e-002$	0.92098	$1.280e-002$
0.025	0.58367	$6.285e-003$	0.85088	$7.284e-003$	0.75549	$6.761e-003$
0.0125	1.22648	$4.194e-003$	1.16427	$4.038e-003$	1.29260	$4.005e-003$
0.00625	0.65763	$1.792e-003$	0.83753	$1.802e-003$	0.73386	$1.635e-003$
0.003125	1.50268	$1.136e-003$	1.12176	$1.008e-003$	1.50429	$9.830e-004$

Table 3 Errors of the approximation schemes Godunov (G), Kinetic of first order ($3VK_1$) and of second order ($3VK_2$) for data (4.6), $T = 1.0$

	G	$3VK_1$	$3VK_2$
h	L^1 Error	L^1 Error	L^1 Error
0.1	$2.07651e-002$	$2.19038e-002$	$2.41712e-002$
0.05	$1.25376e-002$	$1.45365e-002$	$1.35243e-002$
0.025	$8.38778e-003$	$8.07708e-003$	$8.00970e-003$
0.0125	$3.58458e-003$	$3.60392e-003$	$3.26967e-003$
0.00625	$2.27234e-003$	$2.01675e-003$	$1.96603e-003$
0.003125	$8.01899e-004$	$9.26764e-004$	$8.49835e-004$

Notice that $\hat{\gamma}_i, \hat{\gamma}_j$ are the maximized incoming and outgoing fluxes obtained with the procedure described in Sect. 2, where the inversion of the flux function f follows the rules below.

- For roads entering the junction:
  - If $u_L^h \in [0, \sigma]$ and $\hat{\gamma}_i < F(u_L^h)$ then $F^{-1}(\hat{\gamma}_i) \in [\tau(u_L^h), 1)$,
  - If $u_L^h \in [0, \sigma]$ and $\hat{\gamma}_i = F(u_L^h)$ then $F^{-1}(\hat{\gamma}_i) = u_L^h$,
  - If $u_L^h \in [\sigma, 1]$ then $F^{-1}(\hat{\gamma}_i) \in [\sigma, 1]$,

  with $i = 1, 2$;
- For roads coming out of the junction:
  - If $u_0^h \in [\sigma, 1]$ and $\hat{\gamma}_j < F(u_0^h)$ then $F^{-1}(\hat{\gamma}_j) \in [0, \tau(u_0^h))$,
  - If $u_0^h \in [\sigma, 1]$ and $\hat{\gamma}_j = F(u_0^h)$ then $F^{-1}(\hat{\gamma}_j) = u_0^h$,
  - If $u_0^h \in [0, \sigma]$ then $F^{-1}(\hat{\gamma}_j) \in [0, \sigma]$,

  with $j = 1, 2$.

Recall that u_m^h indicates a macroscopic variable and it represents a density.

3.3.3 Conditions at Traffic Light

In order to deal with traffic lights we introduce some suitable boundary conditions for numerical schemes in the point where traffic light is placed along the road, namely x_L. Let $m = m_L$ be the node of the numerical mesh of the discretization corresponding to the traffic light position.

Consider first Godunov method. For the space node on the left of the traffic light we set

$$v_{m_L-1}^{h+1} = v_{m_L-1}^h - \frac{\Delta t}{\Delta x}\big(g^G(v_{m_L-1}^h, 1) - g^G(v_{m_L-2}^h, v_{m_L-1}^h)\big), \tag{3.27}$$

while for the node on the right we have

$$v_{m_L}^{h+1} = v_{m_L}^h - \frac{\Delta t}{\Delta x}\big(g^G(v_{m_L}^h, v_{m_L+1}^h) - g^G(0, v_{m_L}^h)\big). \tag{3.28}$$

« ARCO 11831 layout: Large reference style: basic file: arco9004.tex (Aistes) aid: 9004 doctopic: OriginalPaper class: spr-twocol-v1 v.2007/05/18 Prn:19/05/2007; 13:34 p. 17»

Fig. 15 Traffic can still enter on the left, $h = 0.0125$, $\Delta_g = 1.5$, $\Delta_r = 0.5$, $T = 3.8$

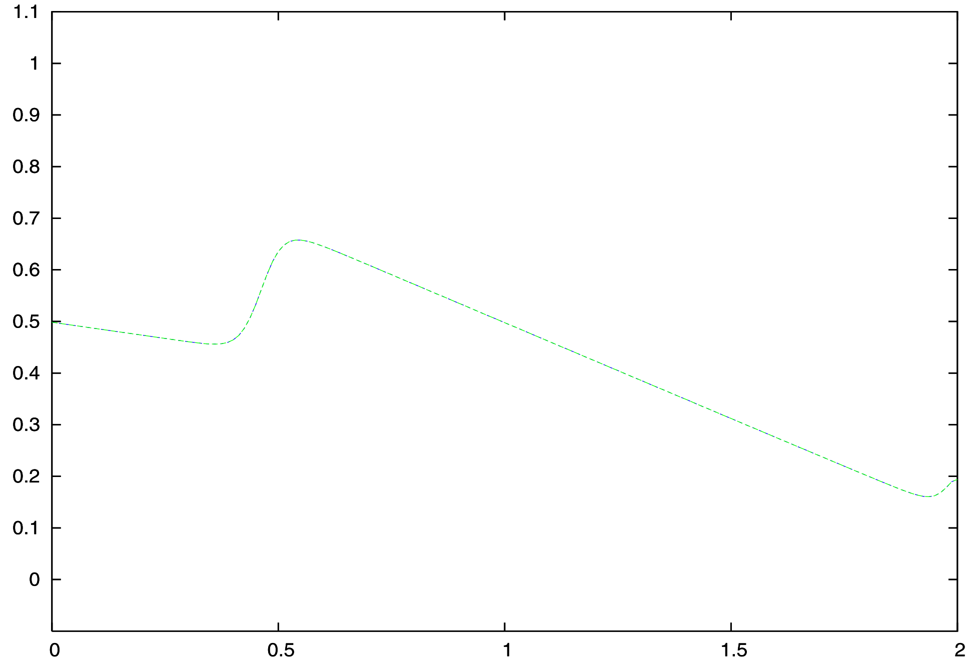

Fig. 16 Evolution in time for data (4.6) computed by $3VK_2$ scheme, $h = 0.0125$

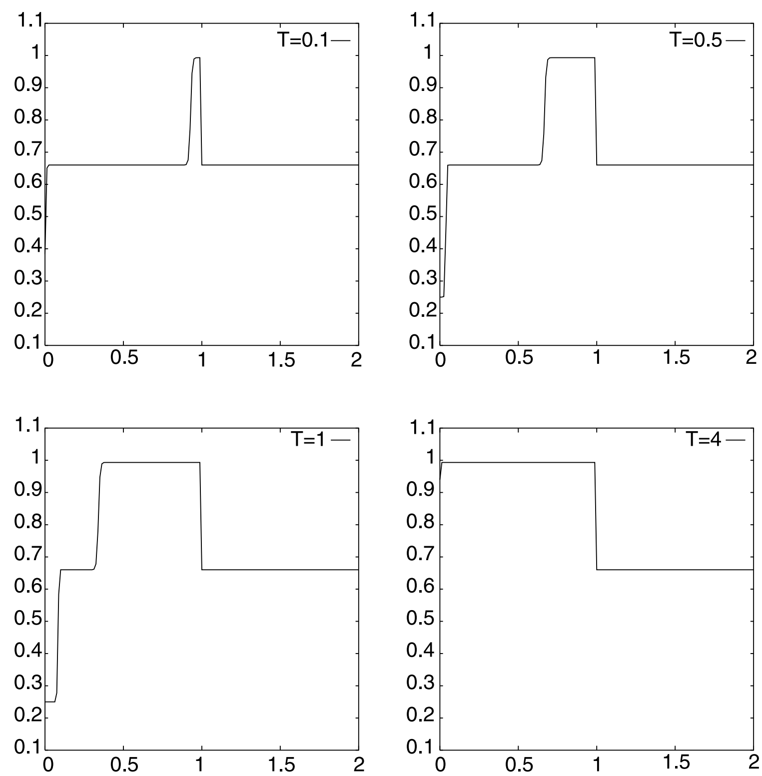

Notice that for the relaxation scheme written in the macroscopic variables the conditions at the traffic lights coincide with the conditions written for the Godunov method.

Let us now turn to the kinetic scheme written in the microscopic variables. At the left boundary respect to the traffic light ($m = m_L - 1$) the scheme reads:

$$f^{h+\frac{1}{2}}_{m_L-1,k} = f^h_{m_L-1,k}(1 - D^h_{m_L-1+\frac{1}{2},k}) + D^h_{m_L-1+\frac{1}{2},k} f^h_{m_L,k}, \quad \text{for } \lambda_k \leq 0, \tag{3.29}$$

where we impose

$$f^h_{m_L,k} = M_k(1).$$

« **ARCO 11831** layout: Large reference style: basic file: arco9004.tex (Aistes) aid: 9004 doctopic: OriginalPaper class: spr-twocol-v1 v.2007/05/18 Prn:19/05/2007; 13:34 p. 18»

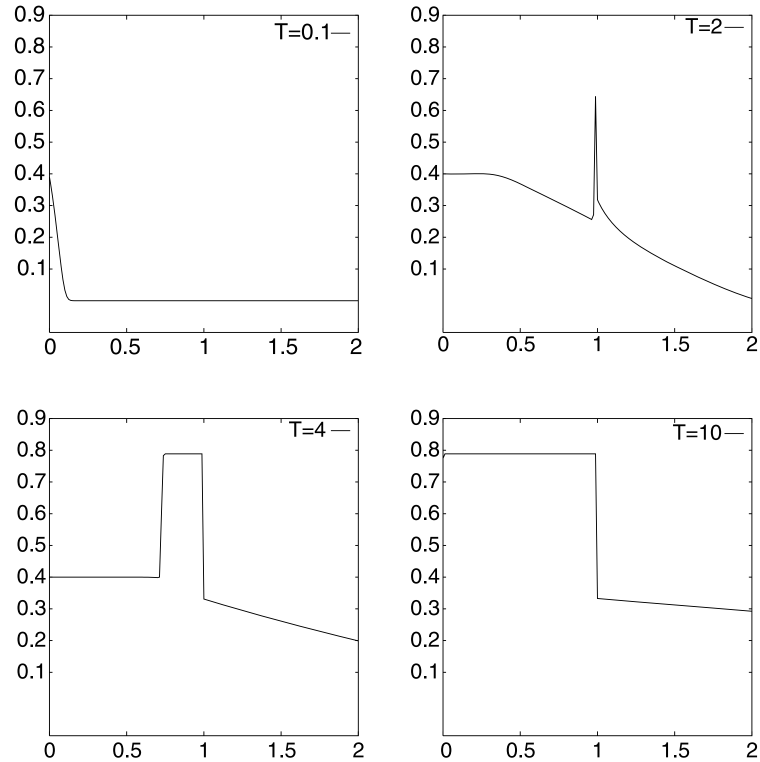

Fig. 17 Evolution in time for data (4.7) computed by $3VK_2$ scheme, $h = 0.0125$

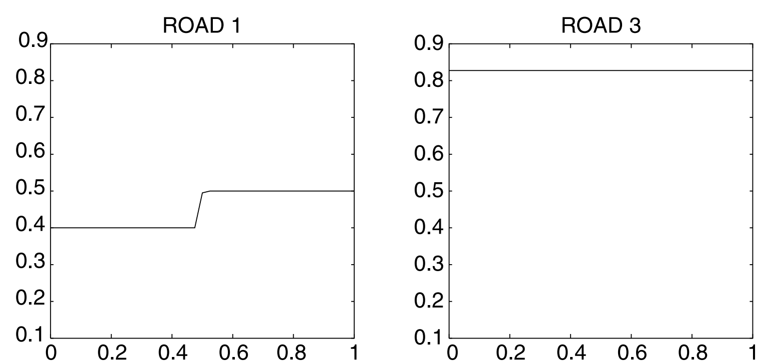

Fig. 18 Initial configuration of data (4.10) with $\rho_1 = 0.4 = \rho_{1,b}$ at time $T = 0$, with $h = 0.025$

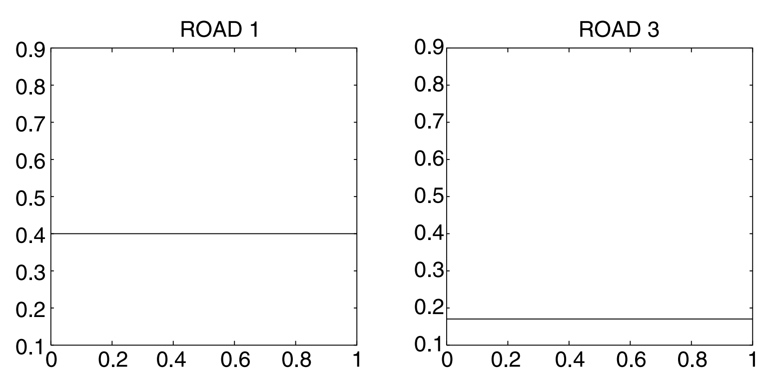

Fig. 19 Situation after the interaction, $T = 25$, $h = 0.025$

« **ARCO 11831** layout: Large reference style: basic file: arco9004.tex (Aistes) aid: 9004 doctopic: OriginalPaper class: spr-twocol-v1 v.2007/05/18 Prn:19/05/2007; 13:34 p. 19»

Fig. 20 Final configuration, $T = 470$, $h = 0.025$

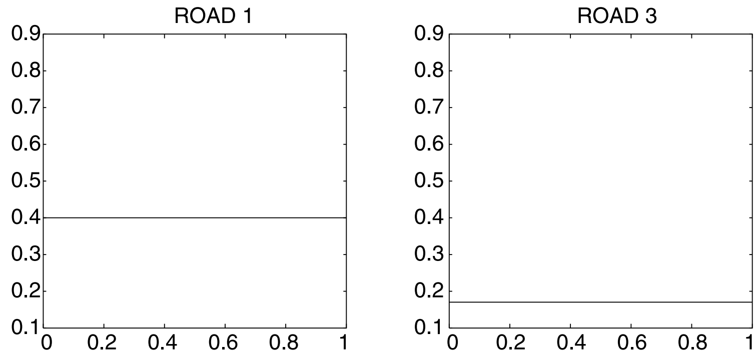

Table 4 Orders and errors of the approximation schemes Godunov (G), Kinetic of first order ($3VK_1$) and of second order ($3VK_2$) for data (4.7), $T = 1$

	G		$3VK_1$		$3VK_2$	
h	γ	L^1 Error	γ	L^1 Error	γ	L^1 Error
0.1	0.65705	$1.841e-002$	0.65705	$1.841e-002$	0.81414	$1.2733e-002$
0.05	0.67659	$1.167e-002$	0.67659	$1.168e-002$	0.82570	$7.2418e-003$
0.025	0.70677	$7.305e-003$	0.70676	$7.306e-003$	0.84143	$4.0859e-003$
0.0125	0.73821	$4.476e-003$	0.73821	$4.476e-003$	0.85393	$2.2803e-003$
0.00625	0.76816	$2.683e-003$	0.76816	$2.683e-003$	0.86470	$1.2616e-004$
0.003125	0.79447	$1.575e-003$	0.79447	$1.575e-003$	0.87441	$6.9283e-004$

Table 5 Errors of the approximation schemes Godunov (G), Kinetic of first order ($3VK_1$) and of second order ($3VK_2$) for data (4.7), $T = 4$

	G	$3VK_1$	$3VK_2$
h	L^1 Error	L^1 Error	L^1 Error
0.1	$2.16316e-002$	$2.18455e-002$	$1.69308e-002$
0.05	$7.10040e-003$	$1.09717e-002$	$1.09403e-002$
0.025	$4.70270e-003$	$5.44031e-003$	$3.70921e-003$
0.0125	$2.48223e-003$	$2.61377e-003$	$2.61455e-003$
0.00625	$1.09907e-003$	$8.57023e-004$	$7.89821e-004$
0.003125	$5.80967e-004$	$3.61744e-004$	$2.75442e-004$

For $\lambda_k \le 0$ we have

$$\sigma^h_{m_L-1,k} = \operatorname{minmod}\left(2\frac{f^h_{m_L,k} - f^h_{m_L-1,k}}{\Delta x}, \frac{f^h_{m_L-1,k} - f^h_{m_L-2,k}}{\Delta x}\right),$$

$$\sigma^h_{m_L,k} = 0,$$

and in the case $\lambda_k > 0$ we set

$$\sigma^h_{m_L-1,k} = f^h_{m_L-1,k} - f^h_{m_L-2,k}.$$

At the right boundary ($m = m_L$) the scheme is

$$f^{h+\frac{1}{2}}_{m_L,k} = f^h_{m_L,k}(1 - D^h_{m_L-\frac{1}{2},k}) + D^h_{m_L-\frac{1}{2},k}\, f^h_{m_L-1,k}, \quad \text{for } \lambda_k > 0, \tag{3.30}$$

where we impose

$$f^h_{m_L-1,k} = M_k(0).$$

For $\lambda_k > 0$ we have

$$\sigma^h_{m_L-1,k} = 0,$$

$$\sigma^h_{m_L,k} = \operatorname{minmod}\left(\frac{f^h_{m_L+1,k} - f^h_{m_L,k}}{\Delta x}, 2\frac{f^h_{m_L,k} - f^h_{m_L-1,k}}{\Delta x}\right),$$

and in the case $\lambda_k <= 0$ we have

$$\sigma^h_{m_L,k} = f^h_{m_L+1,k} - f^h_{m_L,k}.$$

4 Tests

In this section we present some numerical tests performed with the schemes previously introduced, such as the Godunov scheme (G), the three-velocities Kinetic scheme of first order ($3VK_1$) and the three-velocities Kinetic method of second order ($3VK_2$) with $\lambda_3 = -\lambda_1 = 1.0$ and $\lambda_2 = 0$. In general, the three-velocities kinetic models work better than the two-velocities ones. We introduce the formal order of convergence γ of a numerical method as an average on

Table 6 Convergence order γ and errors of the approximation schemes Godunov (G), kinetic 3-velocities of first order ($3VK_1$) and second order ($3VK_2$), for $T=1$

	G		$3VK_1$		$3VK_2$	
h	γ	L^1 Error	γ	L^1 Error	γ	L^1 Error
0.2	1.4	$6.01235e-003$	1.4	$6.00949e-003$	1.9	$6.72896e-003$
0.1	0.88	$2.27825e-003$	0.88	$2.27511e-003$	0.94	$1.82122e-003$
0.05	0.93	$1.23890e-003$	0.93	$1.23605e-003$	0.98	$9.49608e-004$
0.025	0.97	$6.51197e-004$	0.98	$6.48354e-004$	0.99	$4.81271e-004$
0.0125	0.98	$3.32129e-004$	0.99	$3.29293e-004$	0.99	$2.41161e-004$
0.00625	0.98	$1.67647e-004$	1.0	$1.65002e-004$	1.0	$1.20602e-004$

Table 7 L^1-errors of the approximation schemes Godunov (G), kinetic 3-velocities of first order ($3VK_1$) and second order ($3VK_2$) obtained using the exact solution at time $T=20$

	G	$3VK_1$	$3VK_2$
h	L^1 Error	L^1 Error	L^1 Error
0.2	$1.11248e-001$	$5.58553e-002$	$5.53875e-002$
0.1	$4.56467e-002$	$2.24683e-002$	$2.07874e-002$
0.05	$1.21337e-002$	$9.74289e-003$	$6.93735e-003$
0.025	$1.17982e-002$	$5.76965e-003$	$5.41827e-003$
0.0125	$1.16302e-002$	$8.02476e-003$	$8.04770e-003$
0.00625	$7.44115e-003$	$5.62481e-003$	$5.63628e-003$

the set of roads N, where N is the total amount of roads in the network:

$$\gamma = \frac{1}{N}\sum_{i=1}^{N}\gamma_i, \tag{4.1}$$

where

$$\gamma_i = \log_2\left(\frac{e^i(1)}{e^i(2)}\right), \quad i=1,\dots,N, \tag{4.2}$$

with i the index of roads composing the network. The L^1-error on each road is

$$e^i(p) = \frac{\Delta x}{p}\sum_{l=0,\dots,pL}\left|w_l^{pM}\left(\frac{\Delta x}{p}\right) - w_{2l}^{pM}\left(\frac{\Delta x}{2p}\right)\right|,$$
$$p=1,2, i=1,\dots,N, \tag{4.3}$$

where $w_m^M(\Delta x)$ denotes the numerical solution obtained with the space step discretization equal to Δx, computed in x_m at the final time $t_M = T$. The total L^1-error is

$$TOT_{\mathrm{err}} = \sum_{i=1}^{N} e^i(1). \tag{4.4}$$

For some animations, see [6].

4.1 Traffic Light

At $t=0$ the light is assumed to be red and, for simplicity, we fix $\Delta_g = \Delta_r = 1.0$ (recall the definitions of Sect. 2.4.1).

Let us assume on the road the following initial and boundary data:

$$\rho(x,0) = 0.3, \qquad \rho_b(t) = 0.5. \tag{4.5}$$

Approximate solutions are computed by three methods, such as Godunov scheme (G), three velocities kinetic method of first order ($3VK_1$) and three velocities kinetic method of second order ($3VK_2$).

At $t=0$ the light is red, thus the density becomes high at $x=1.0$, where the traffic light is placed and there is the generation of a shock propagating backwards, see Fig. 11.

After the light turns green, cars can go and this corresponds to the creation of a rarefaction wave in the direction of traffic flow, as showed in Fig. 12. When the light becomes red, a shock is again produced in correspondence of the point where is placed the traffic light, see Fig. 13, and after a short time we can observe a big value of the car density at the entrance of the road, as depicted in Fig. 14. Considering again the data (4.5) and taking $\Delta_g = 1.5$ and $\Delta_r = 0.5$, thus meaning that the time of green is three times the time of red, one can see that at time $T = 3.8$ the value of density is much lower than in precedence, as showed by Fig. 15.

In Table 1 are reported order and errors for the approximate solution computed with the following methods, such as the Godunov scheme (G), three velocities Kinetic method of first order ($3VK_1$) and three velocities Kinetic method of second order ($3VK_2$). The initial and boundary data are (4.5) and we set $\Delta_g = \Delta_r = 1.0$.

From this simple example it is easy to see that tuning the values Δ_g, Δ_r it is possible to control traffic.

4.2 Bottleneck

Now we want to present some numerical approximations to (2.1) with fluxes (2.15) and (2.16). Tables 2–5 provide a

« **ARCO 11831** layout: Large reference style: basic file: arco9004.tex (Aistes) aid: 9004 doctopic: OriginalPaper class: spr-twocol-v1 v.2007/05/18 Prn:19/05/2007; 13:34 p. 21»

Table 8 Convergence order γ, defined in (4.1), and errors of the approximation schemes Godunov (G), 3 velocities Kinetic methods of first order ($3VK_1$) and of second order ($3VK_2$) for data 4.11, $q = 0.25$, $T = 1$

	G		$3VK_1$		$3VK_2$	
h	γ	L^1 Error	γ	L^1 Error	γ	L^1 Error
0.1	0.738593	0.009851	0.792745	0.009130	1.458312	0.009001
0.05	0.839375	0.005904	0.879531	0.005270	1.560714	0.003214
0.025	0.895055	0.003300	0.936022	0.002865	1.581739	0.000812
0.0125	0.929770	0.001774	0.968897	0.001497	1.524962	0.000473
0.00625	0.952295	0.000931	0.985818	0.000765	1.572714	0.000101
0.003125	0.983923	0.000481	0.9972134	0.000386	1.560145	0.000072

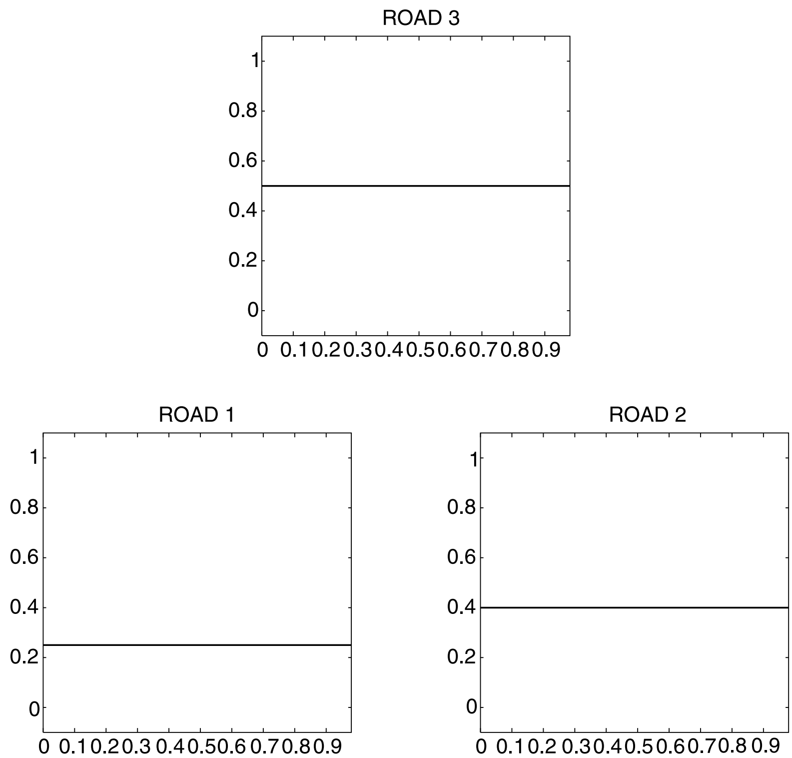

Fig. 21 1 outgoing and 2 incoming roads with $q = 0.5$, $h = 0.0125$, $T = 0$

comparison between the three methods in terms of L^1-error (4.3) and order of convergence (4.1).

Here we deal with a road of length 2 parametrized by the interval $[0, 2]$ with the separation point placed in the middle of the road, namely $x = 1$. The numerical schemes used to provide the approximate solution are Godunov scheme (G), three-velocities Kinetic scheme of first order ($3VK_1$) and second order ($3VK_2$) with the following velocities: $\lambda_3 = -\lambda_1 = 1.0$ and $\lambda_2 = 0$.

Test B1 Let us take the following initial and boundary data

$$\begin{aligned} &\rho_1(0, x) = 0.66, \qquad \rho_2(0, x) = 0.66, \\ &\rho_1(t, 0) = \rho_{1,b}(t) = 0.25. \end{aligned} \tag{4.6}$$

Since the initial value 0.66 is very close to the maximum value that can be absorbed by road 2, after a short time, namely $T = 2$, the formation of a traffic jam can be observed, see Fig. 16. Orders and errors are given in Tables 2 and 3.

Test B2 Let us assume the road is initially empty and take the following initial and boundary data

$$\rho_1(0, x) = \rho_2(0, x) = 0, \qquad \rho_{1,b}(t) = 0.4. \tag{4.7}$$

Since $\rho_{1,b} > \bar{\rho} \simeq 0.21$, even in this case there is a jam formation, as explained in Sect. 2.4.2, see Fig. 17. Orders and errors are given in Tables 4 and 5.

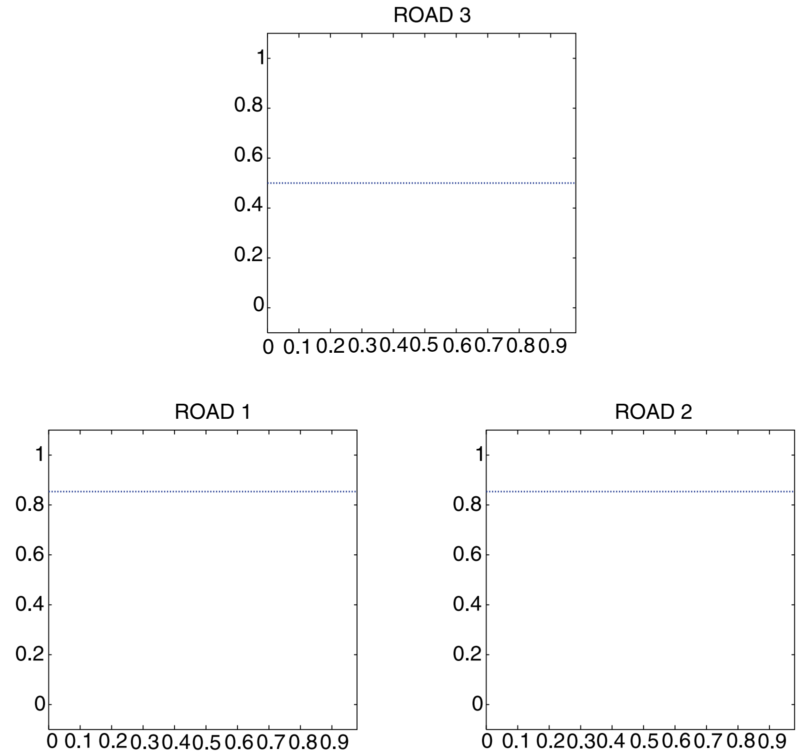

Fig. 22 1 outgoing and 2 incoming roads with $q = 0.5$, $h = 0.0125$, $T = 10$

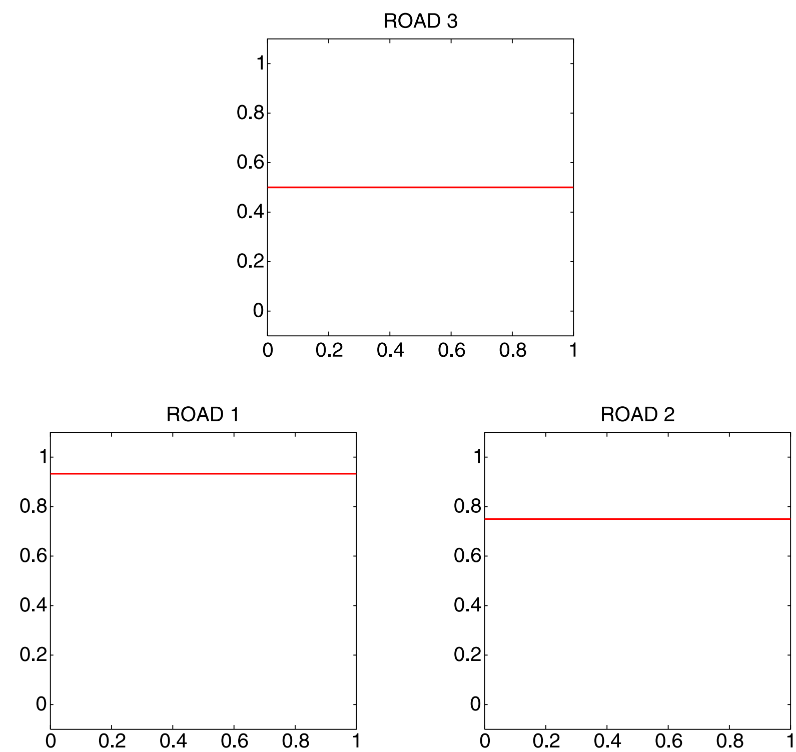

Fig. 23 1 outgoing and 2 incoming roads with $q = 0.25$, $h = 0.0125$, $T = 10$

From the analysis of the previous tables we can see that both $3VK_1$ and $3VK_2$ perform better than the Godunov scheme. In fact, the kinetic schemes show a good stability even after the interaction at the junction.

4.3 Two Incoming–Two Outgoing Roads

Recall definitions of Sect. 2.4 of junction J with two incoming roads and two outgoing roads all parametrized with the interval $[0, 1]$. Here we refer to the situation described in

« **ARCO 11831** layout: Large reference style: basic file: arco9004.tex (Aistes) aid: 9004 doctopic: OriginalPaper class: spr-twocol-v1 v.2007/05/18 Prn:19/05/2007; 13:34 p. 23»

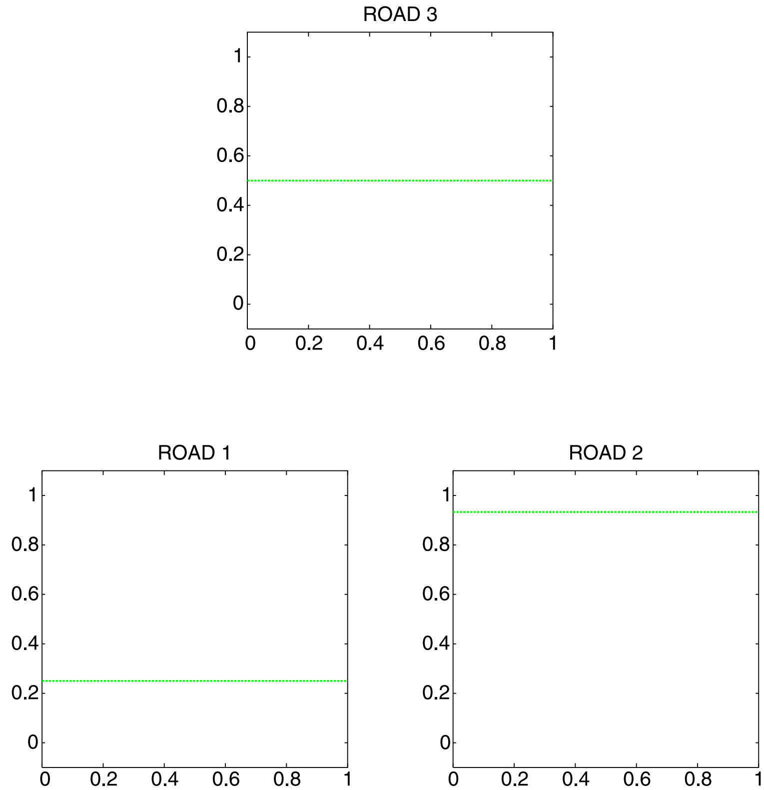

Fig. 24 1 outgoing and 2 incoming roads with $q = 0.75$, $h = 0.0125$, $T = 10$

Appendix of [9], where the coefficients of the distribution matrix A are such that $0 < \alpha_{32} < \alpha_{31} < 1/2$. We set

$$\alpha_{31} = \alpha_1, \qquad \alpha_{32} = \alpha_2, \qquad \alpha_{41} = 1 - \alpha_1,$$
$$\alpha_{42} = 1 - \alpha_2$$

and we introduce the notation

$$\rho_1(0,x) = \rho_{1,0}, \qquad \rho_2(0,x) = \rho_{2,0}, \qquad \rho_3(0,x) = \rho_{3,0},$$
$$\rho_4(0,x) = \rho_{4,0}.$$

The flux function is taken as in (3.2) and the distribution matrix is fixed as

$$A = \begin{pmatrix} 0.4 & 0.3 \\ 0.6 & 0.7 \end{pmatrix} \tag{4.8}$$

We assume the following constant initial and boundary data

$$\begin{aligned} &\rho_{1,0} = \rho_{4,0} = \sigma, \\ &\rho_{2,0} = \rho_{3,0} = f^{-1}\left(\frac{\alpha_1}{1-\alpha_2} f(\sigma)\right) = 0.82732683535, \\ &\rho_{1,b}(t) = \sigma, \\ &\rho_{2,b}(t) = f^{-1}\left(\frac{\alpha_1}{1-\alpha_2} f(\sigma)\right) = 0.82732683535. \end{aligned} \tag{4.9}$$

Remark 4.1 Notice that the boundary condition is imposed only on the incoming roads, as for the outgoing ones we use a Neumann condition at the final endpoint.

Let us introduce a perturbation on the initial data of road 1

$$\rho_1(0,x) = \begin{cases} \rho_{1,0} = \sigma & \text{if } 0 \le x \le 0.5, \\ \rho_1 & \text{if } x \ge 0.5, \end{cases} \tag{4.10}$$

and ρ_1, $\rho_{1,0}$, $\rho_{2,0}$, $\rho_{3,0}$, $\rho_{4,0}$ be as in (4.9), so that ($\rho_{1,0}$, $\rho_{2,0}$, $\rho_{3,0}$, $\rho_{4,0}$) is an equilibrium configuration.

In (4.10) assume to have a small perturbation, represented by $\rho_1 = 0.4$, and let the boundary data on road 1 be $\rho_{1,b} = 0.4$. The initial and boundary data on the other roads are taken as in (4.9). After a certain time ($t \sim 8$) the wave $(\rho_1, \rho_{1,0})$ interacts with the junction thus determining a shock wave travelling on road 3. At time $T = 470$ a new equilibrium configuration is reached: the value of density on road 4 remains constant and on road 2 the final density is very close the initial value $\rho_{2,0}$. In Figs. 18–20 we describe the evolution in time of road 1 and road 3, where numerical solutions were produced by the $3VK_2$ scheme. Tables 6 and 7 report orders and L^1-errors of the schemes, defined by (4.1), respectively before and after the interaction at the junction. Looking at Table 7 one can observe that the accuracy of kinetic methods is higher respect to Godunov scheme. This reveals that Godunov scheme is more diffusive. Notice that in this case for $3VK_2$ scheme we used the boundary condition $\sigma^h_{0,k} = 0$ for $\lambda_k < 0$.

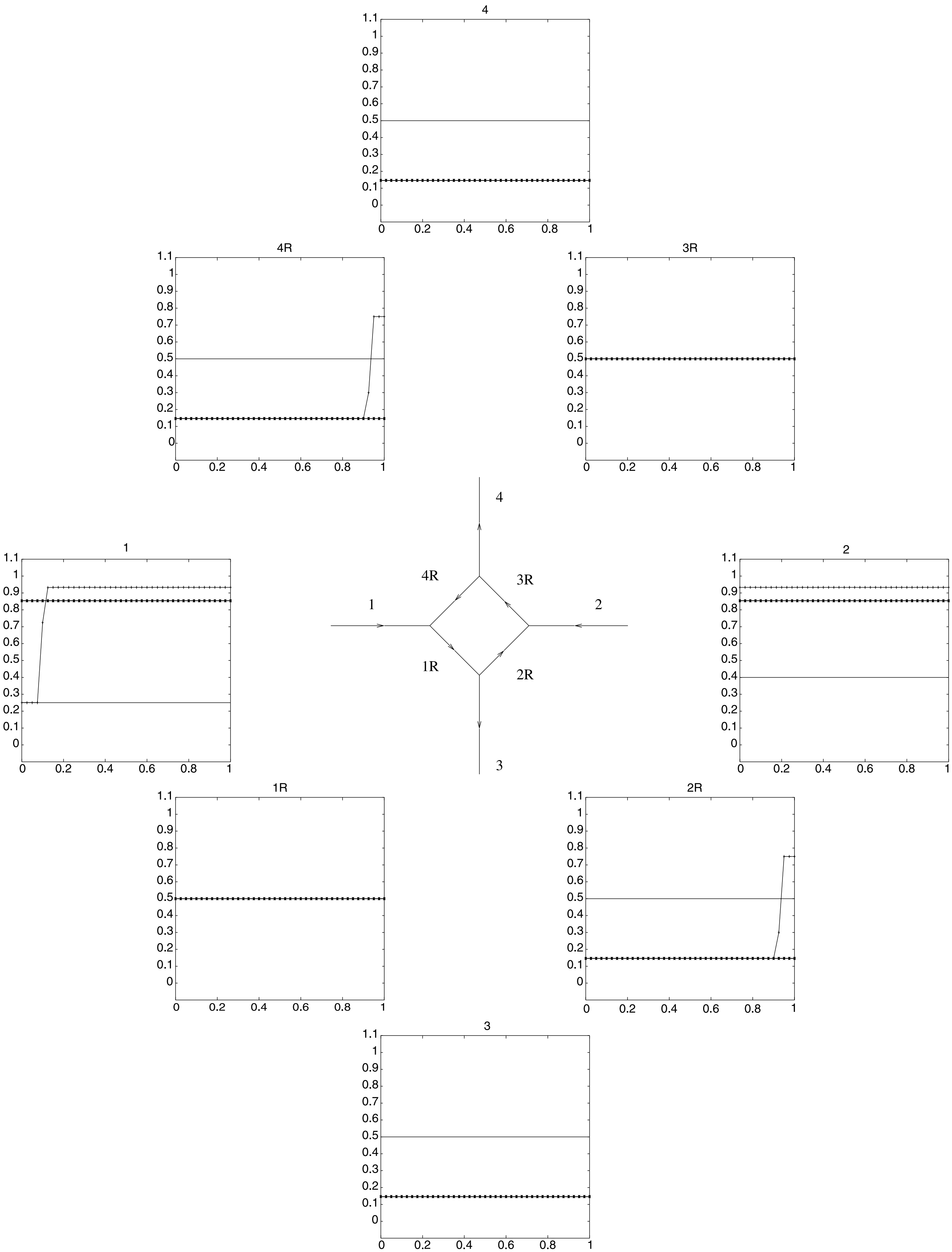

Fig. 25 Traffic circle with $q_1 = q_2 = 0.25$

« ARCO 11831 layout: Large reference style: basic file: arco9004.tex (Aistes) aid: 9004 doctopic: OriginalPaper class: spr-twocol-v1 v.2007/05/18 Prn:19/05/2007; 13:34 p. 25»

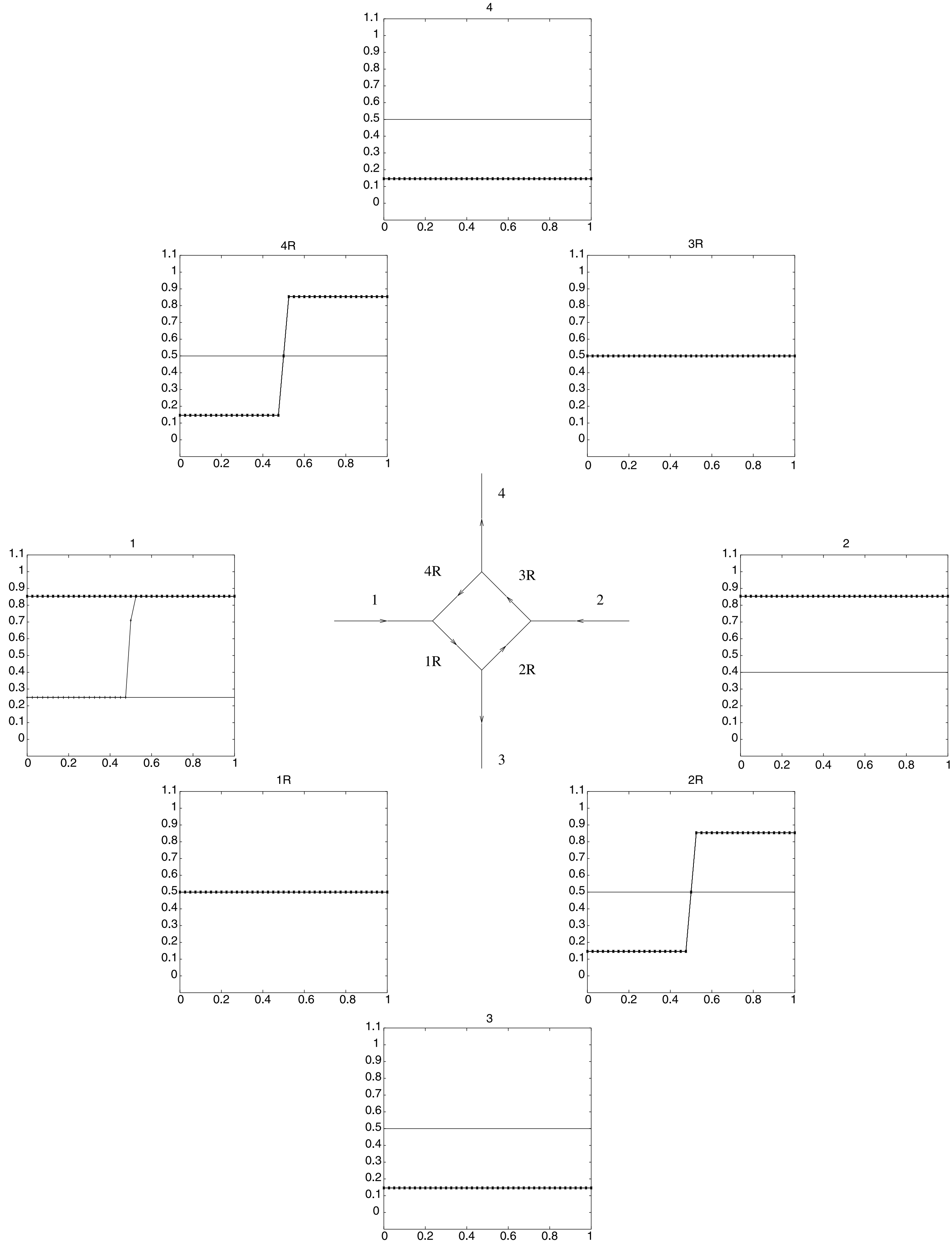

Fig. 26 Traffic circle with $q_1 = q_2 = 0.5$

« **ARCO 11831** layout: Large reference style: basic file: arco9004.tex (Aistes) aid: 9004 doctopic: OriginalPaper class: spr-twocol-v1 v.2007/05/18 Prn:19/05/2007; 13:34 p. 26»

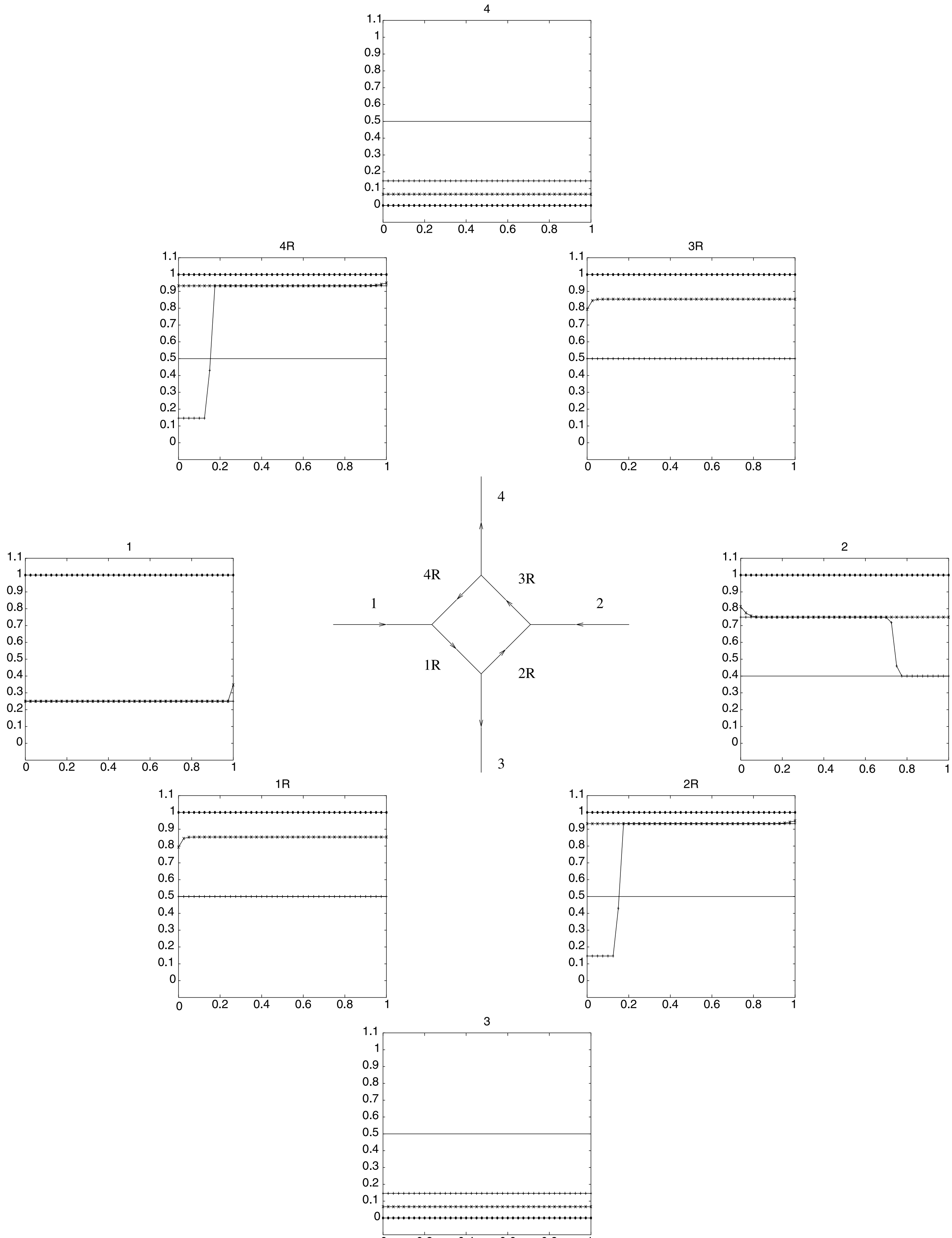

Fig. 27 Traffic circle with $q_1 = q_2 = 0.75$

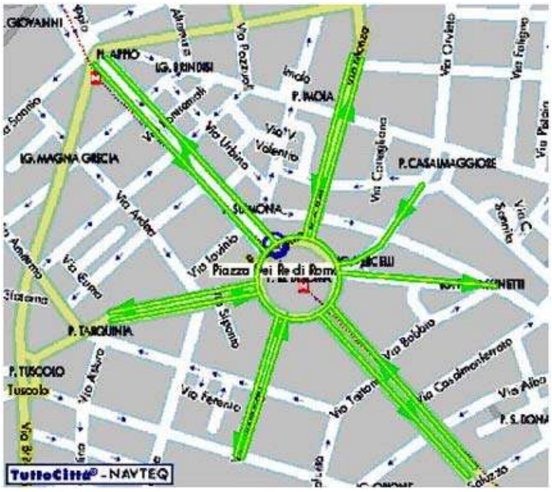

Fig. 28 Re di Roma

4.4 Junction with 2 Incoming and 1 Outgoing Roads

Recall rule (C) of Sect. 2. Consider a crossing with two incoming roads and one outgoing road all parametrized by [0, 1] and fix a right of way parameter $q \in]0, 1[$.

$$\begin{aligned} &\rho_{1,0} = 0.25, \qquad \rho_{2,0} = 0.4, \qquad \rho_{3,0} = 0.5, \\ &\rho_{1,b}(0,t) = 0.25, \qquad \rho_{2,b}(0,t) = 0.4. \end{aligned} \tag{4.11}$$

In Figs. 21–24 we represent road 3 in the upper graph, road 1 on the lower left graph and road 2 on the lower right one. The numerical solutions have been generated by Godunov method.

The initial data is depicted in Fig. 21.

First we take $q = 0.5$ (see Fig. 22). Both the incoming roads have the same right of way parameter: the density increases on road 1 and road 2 and becomes considerably high, while the density on road 3 remains constant.

Then assume $q = 0.25$ and observe the situation described in Fig. 23. In the case represented in Fig. 23 road 2 has the right of way parameter equal to $1 - q = 0.75$. It is easy to see that the density becomes very high on road 1, since road 2 has the priority to pass; the density is high on road 2 and remains the same on road 3.

Now take $q = 0.75$. Figure 24 shows that road 1 preserves its value of density, together with road 3, while road 2 reaches a very high value of density, due to the fact that its right of way parameter is $1 - q = 0.25$.

In Table 8 are reported orders and errors for data (4.11).

4.5 Traffic Circles

In the next pages we present some simulations reproducing a simple traffic circle composed by 8 roads and 4 junctions. The numerical solutions have been generated by the $3VK_2$ method for $h = 0.025$ and $CFL = 0.5$.

Consider the following initial and boundary data

$$\begin{aligned} &\rho_1(0,x) = 0.25, \qquad \rho_2(0,x) = 0.4, \\ &\rho_3(0,x) = 0.5, \qquad \rho_4(0,x) = 0.5, \\ &\rho_{1R}(0,x) = 0.5, \qquad \rho_{2R}(0,x) = 0.5, \\ &\rho_{3R}(0,x) = 0.5, \qquad \rho_{4R}(0,x) = 0.5, \\ &\rho_{1,b}(t) = 0.25, \qquad \rho_{2,b}(t) = 0.4. \end{aligned} \tag{4.12}$$

The distribution coefficients, namely $(\alpha_{1R,3}, \alpha_{1R,2R}, \alpha_{3R,4}, \alpha_{3R,4R})$, are assumed to be constant and are all equal to $\alpha = 0.5$. Let us choose the following priority parameters, which are $q_1 = q(1, 4R, 1R) = 0.25$, $q_2 = q(2, 2R, 3R) = 0.25$. The fixed values imply that road $4R$ is the through street respect to road 1 and road $2R$ is the through street respect to 2. The evolution in time of traffic is reported in Fig. 25. Observe that at time $t = 5$ shocks are generated on the entering roads 1 and 2, while rarefaction waves in the direction of traffic are created on roads $4R$, $2R$, 3, 4. Roads $1R$ and $3R$ do not change the level of the density. At $t = 10$ rarefaction waves travelling in the sense of traffic produce a decrease in the car density on roads $4R$, $3R$, 3, 4. On entering roads 1 and 2 the effect of shocks travelling backwards is a considerable increase of the density and, again, roads $1R$ and $3R$ have the same configuration, which corresponds to the maximum flux. At time $T = 40$ the roads entering in the circle have an high value of density as they wait at the junctions, while densities of roads in the circle are lowered due to the fact that traffic is flowing towards the outgoing roads 3 and 4. We can observe that starting from the same configuration (4.12) but setting differently the right of way parameters, traffic within the circle is fluid and is distributed between the outgoing roads.

Figure 26, obtained for data (4.12) and $q_1 = q_2 = 0.5$, shows a situation quite similar to that in Fig. 25. The difference is represented by the values of density on the roads $2R$ and $4R$ that reveal a shock formation with zero speed. As a consequence, the time for covering the path of the circle from road 1 to road 4 is higher than in the case depicted in Fig. 25. In particular, let δ be the portion of road $2R$ at the lowest value of density, i.e. 0.15, and $1 - \delta$ the other portion of the same road, we can estimate the time for covering the path from road 1 to road 4. In the first case is

$$\frac{1}{0.5} + \frac{1}{0.85} + \frac{1}{0.5} \sim 5.17$$

while here (with $\delta = 0.5$) we get

$$\frac{1}{0.5} + \frac{\delta}{0.85} + \frac{1-\delta}{0.15} + \frac{1}{0.5} \sim 7.92$$

and the difference between the previous and the current case is

$$\Delta t = \frac{1-\delta}{0.15} - \frac{1-\delta}{0.85} = (1-\delta)\frac{80}{17},$$

Fig. 29 Re di Roma simulation, $t = 0.25$, $h = 0.01$, $cfl = 0.5$

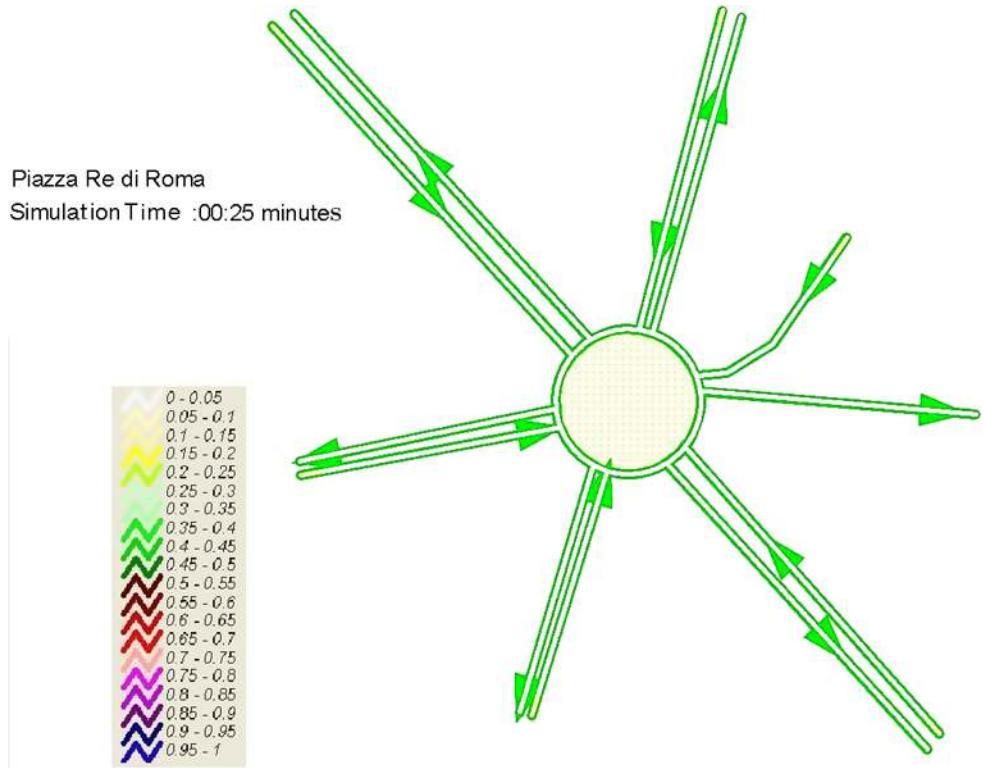

Fig. 30 Re di Roma simulation, $t = 6.25$, $h = 0.01$, $cfl = 0.5$

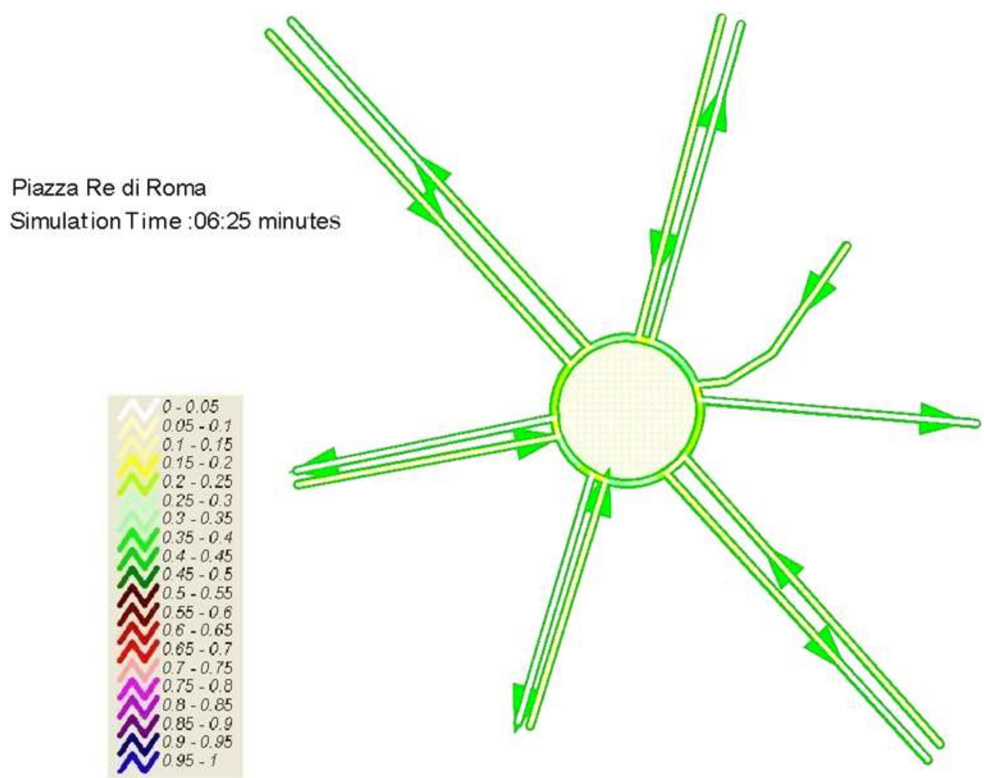

« ARCO 11831 layout: Large reference style: basic file: arco9004.tex (Aistes) aid: 9004 doctopic: OriginalPaper class: spr-twocol-v1 v.2007/05/18 Prn:19/05/2007; 13:34 p. 29»

Fig. 31 Re di Roma simulation, $t = 9.25$, $h = 0.01$, $cfl = 0.5$

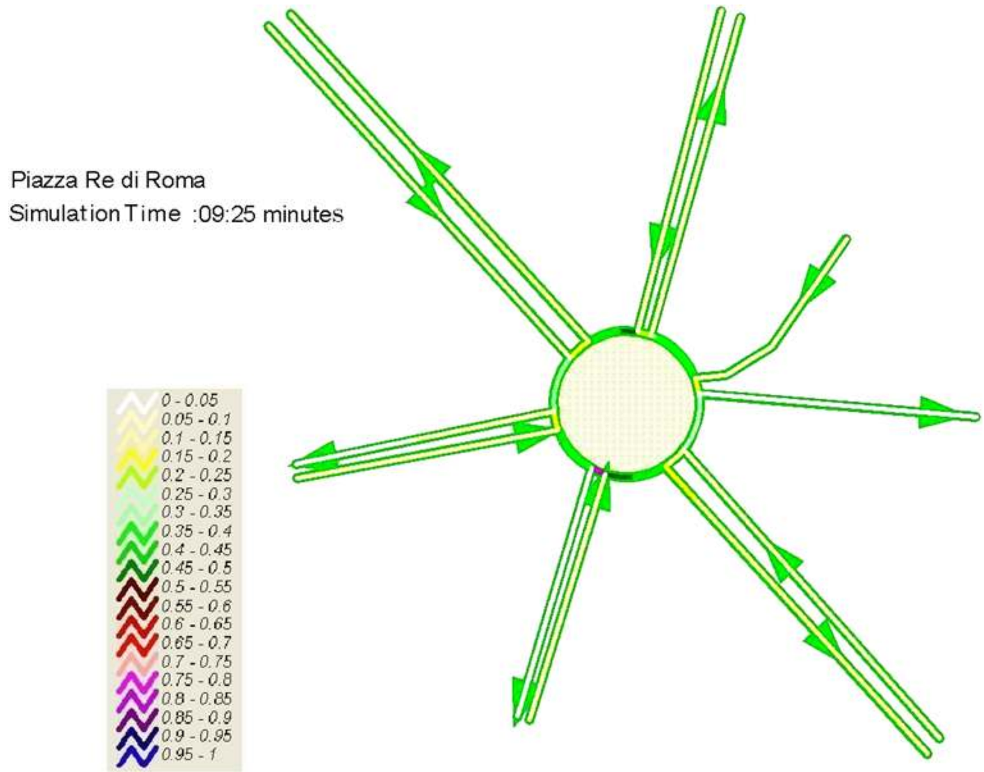

Fig. 32 Re di Roma simulation, $t = 12.25$, $h = 0.01$, $cfl = 0.5$

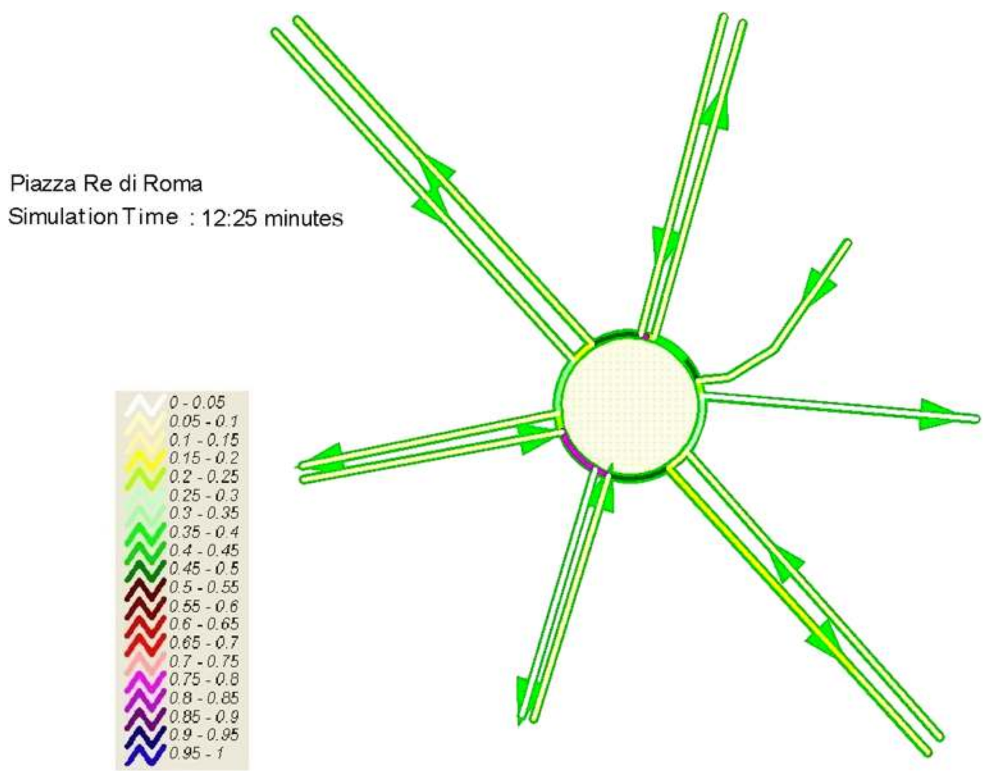

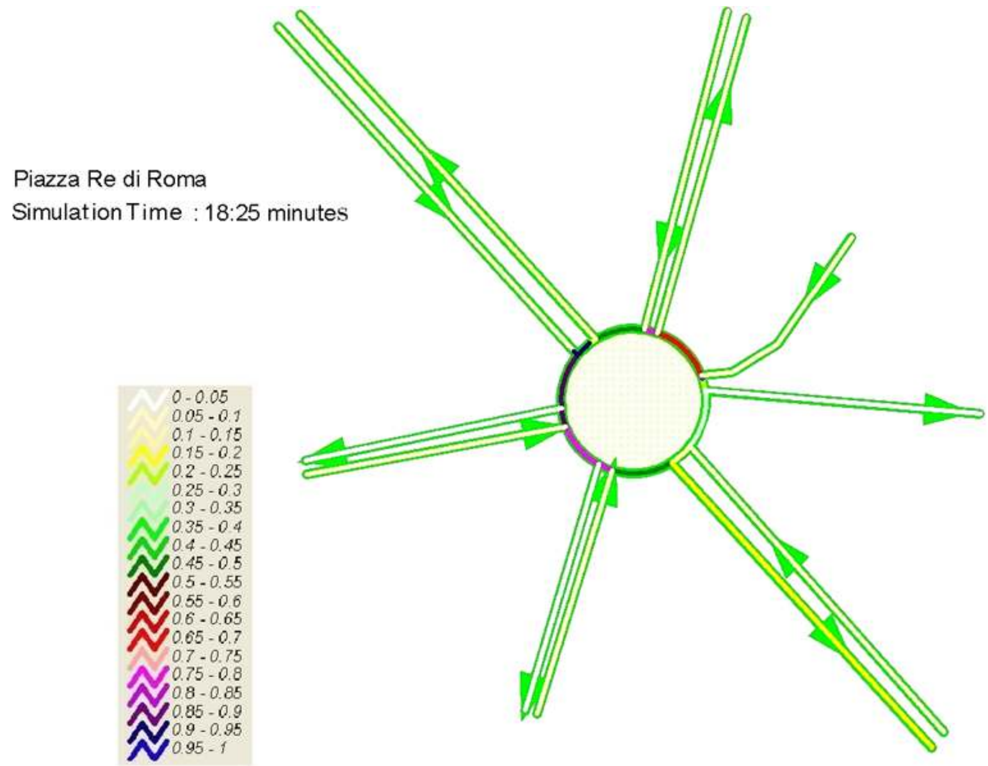

Fig. 33 Re di Roma simulation, $t = 18.25$, $h = 0.01$, $cfl = 0.5$

that is greater as $\delta \to 0$.

Let us set the right of way parameters as $q_1 = q(1, 4R, 1R) = 0.75, q_2 = q(2, 2R, 3R) = 0.75$. This means that road 1 is the through street respect to road $4R$ and road 2 is the through street respect to $2R$. As before, the distribution coefficients are assumed to be constant and all equal to $\alpha = 0.5$. The evolution in time of traffic densities is described in Fig. 27. One can observe that at time $t = 1.5$ the chosen right of way parameters provoke shocks propagating backwards along roads $2R$ and $4R$ and consequently a shock is created on road 2. Successively, the density on roads $4R$, $2R$ increases and shocks are propagating backwards on roads $1R$ and $3R$. Roads 3 and 4 show a very low density of cars. At $T = 40$ densities on the incoming roads and within the circle (all equal to the maximum value $\rho_{\max} = 1$), represent a situation of traffic jam, the so called bumper-to-bumper traffic. This means that no cars can exit the circle, as showed by the fact that roads 3 and 4 are empty. Hence, in that case, the choice of the right of way parameter determines a situation of completely blocked traffic.

Figures 25–27 show the evolution in time of the density for the discussed cases with the following legend:

Legend	
$t = 0$	———
$t = 5$	—+—
$t = 10$	—×—
$t = 40$	—⊟—

Fig. 34 Map of the Salerno junction on the A3 highway

Re di Roma Square Let us now take a portion of urban network. In particular, we consider a crucial area for traffic in the city of Rome, which is represented by the Square of "Re di Roma", showed in Fig. 28. Some animations can be found on the web page [6].

Note that in this case we deal with a network composed by 24 roads and 12 junctions. The next figures show some simulations performed by the Godunov scheme with space step $h = 0.01$, *CFL* 0.5, final time $T = 20$. The network is initially empty and on each incoming road we put a low

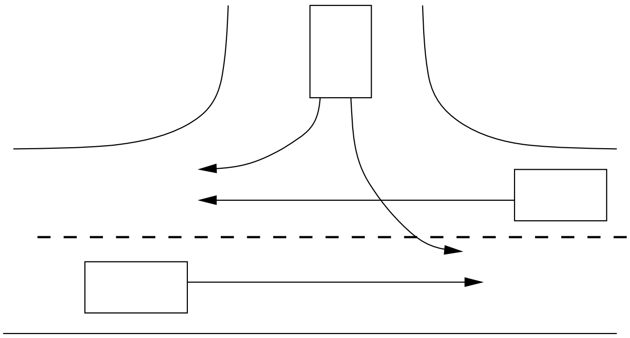

Fig. 35 The junction on the A3 highway

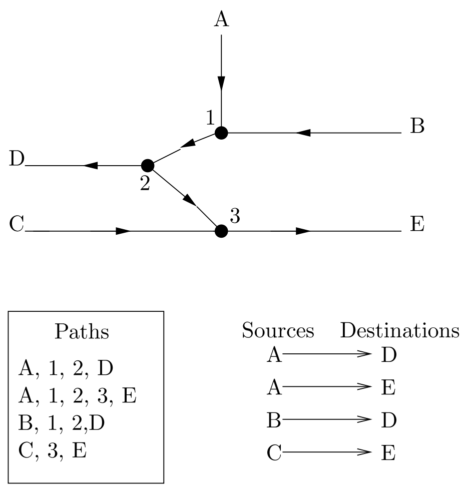

Fig. 36 Schematization of the junction on the A3 highway

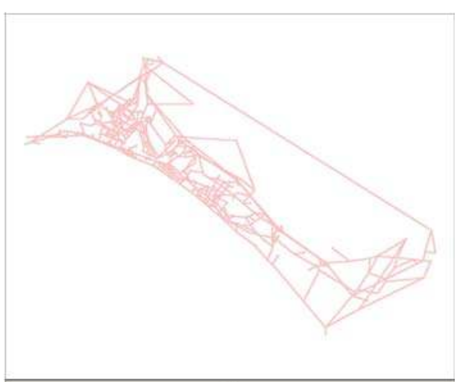

Fig. 37 The entire network of the city

boundary density equal to $\rho_b = 0.1$. The right of way parameters, necessary for the junctions with only one outgoing road, are fixed as $q = 0.5$, while the distribution coefficients are chosen taking into account the different importance between the roads composing the circle. The evolution of densities can be individuated through different colours along the roads(light colours correspond to low density, dark colours to high density).

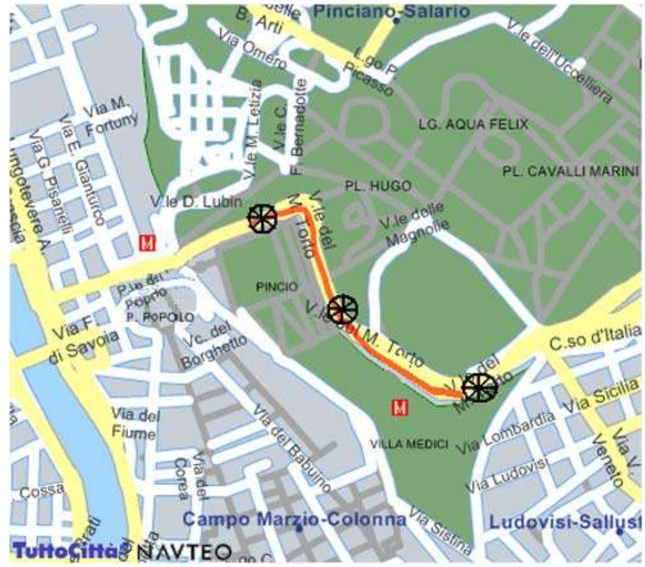

Fig. 38 Viale del Muro Torto

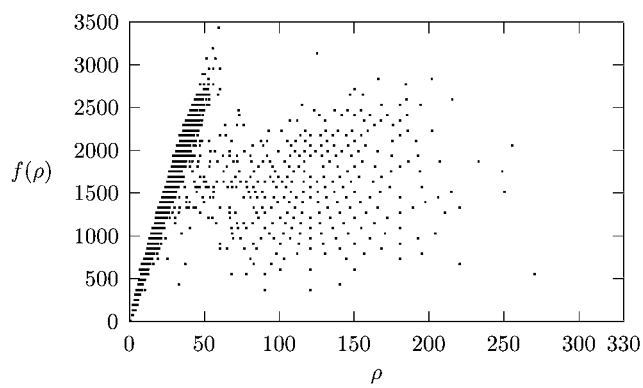

Fig. 39 Measured flux-density diagram

Since at the beginning the network is initially empty, we see that the value of density in the traffic circle for $t = 0.25$ is zero, as underlined by the white color. After a certain time, the traffic on the roads within the circle is congested and the traffic jam starts propagating backwards along the incoming roads.

Salerno Network Some simulations were performed in the area of Salerno on the junction of the A3 highway letting in Via Capone (south direction). A map of the area is depicted in Fig. 34, while in Figs. 35, 36 is represented a schematization of the junction. In particular, if we refer to Fig. 35, the sources are A, B, C while the destinations are D and E. The distribution coefficients for junction 2, which is composed by one incoming and two outgoing roads, are the following:

$$\alpha = \frac{f_{AE}}{f_{BD} + f_{AE} + f_{AD}},$$

« ARCO 11831 layout: Large reference style: basic file: arco9004.tex (Aistes) aid: 9004 doctopic: OriginalPaper class: spr-twocol-v1 v.2007/05/18 Prn:19/05/2007; 13:34 p. 32»

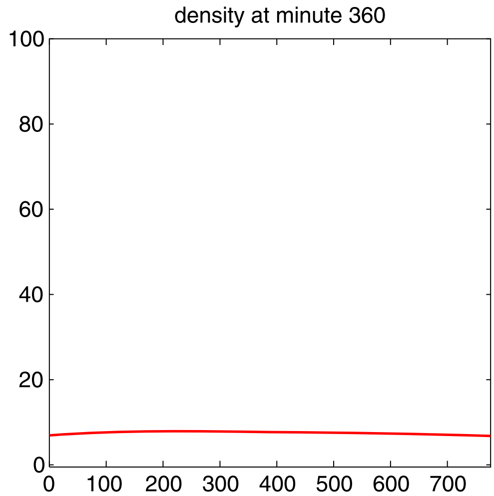

Fig. 40 Density at 6:00

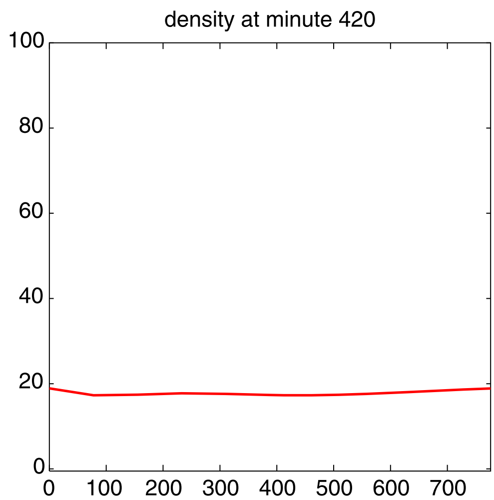

Fig. 41 Density at 7:00

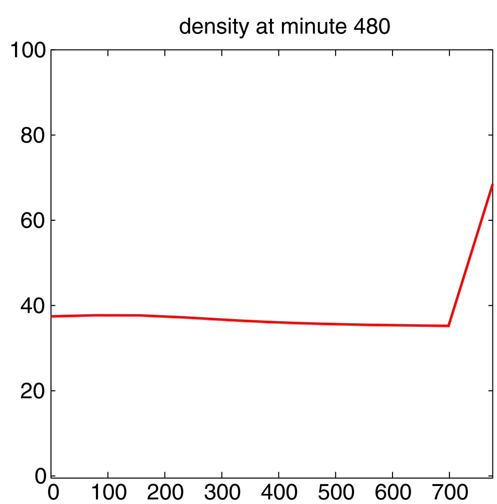

Fig. 42 Density at 8:00

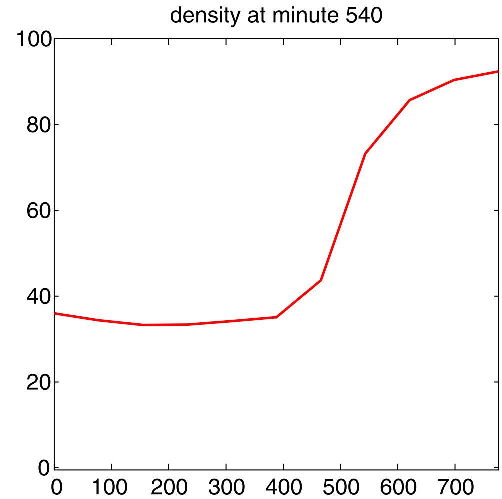

Fig. 43 Density at 9:00

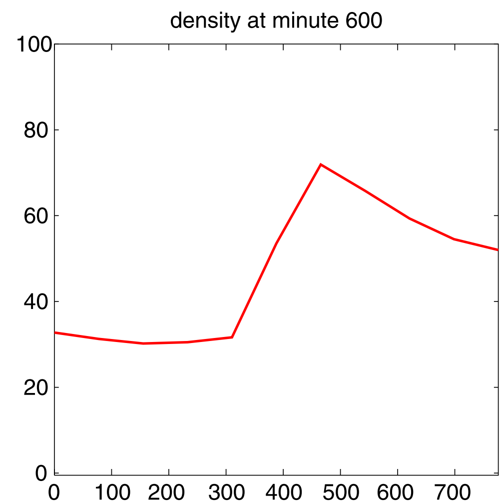

Fig. 44 Density at 10:00

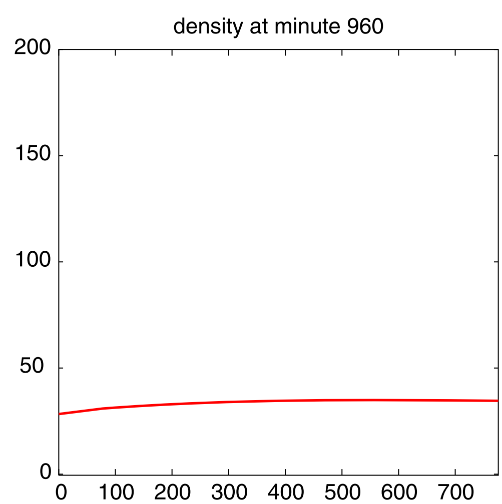

Fig. 45 Density at 16:00

« ARCO 11831 layout: Large reference style: basic file: arco9004.tex (Aistes) aid: 9004 doctopic: OriginalPaper class: spr-twocol-v1 v.2007/05/18 Prn:19/05/2007; 13:34 p. 33»

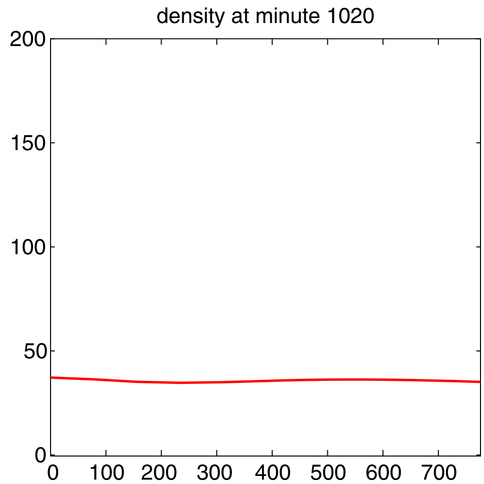

Fig. 46 Density at 17:00

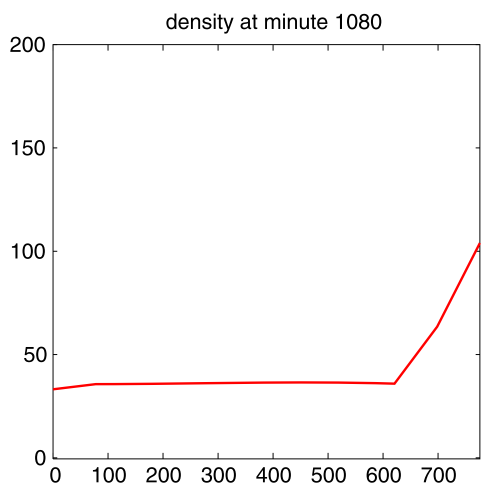

Fig. 47 Density at 18:00

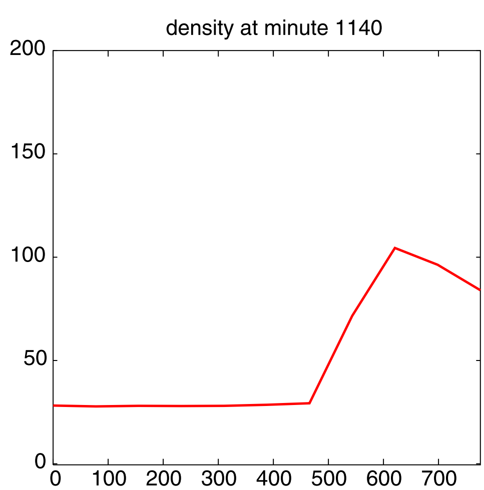

Fig. 48 Density at 19:00

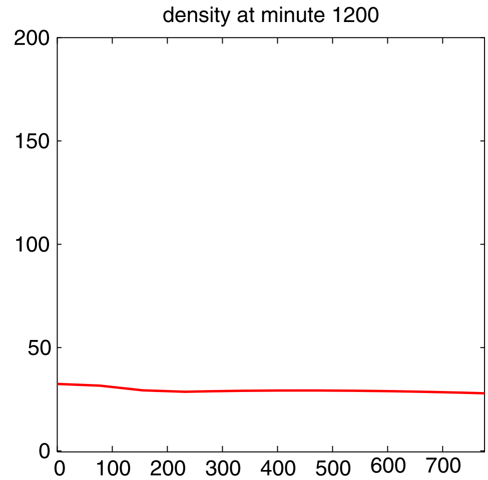

Fig. 49 Density at 20:00

$$1 - \alpha = \frac{f_{BD} + f_{AD}}{f_{BD} + f_{AE} + f_{AD}}$$

with f_{AE}, f_{BD}, f_{AE} the fluxes from the incoming roads (sources) to the outgoing ones (destinations).

We were also able to apply our simulation tool to the entire network of Salerno, represented as a graph composed by about 1500 arcs, see Fig. 37.

Some animations are in [6].

Viale Muro Torto Let us consider another portion of urban network of Rome, namely Viale del Muro Torto in the direction from Corso d'Italia towards Piazza del Popolo.

We compute approximate solutions starting from an empty configuration and using as boundary data experimental data provided by the municipal society for traffic monitoring and control of Rome, namely ATAC S.p.A. Traffic is observed through sensors, located along roads of some areas of the city, which acquire every minute traffic data such as flux, velocity and occupation rate. Approximate solutions of this portion of urban network are computed by Godunov method with boundary conditions given by measured data.

In Fig. 39 we represent a diagram of measured flux during an entire week. The first part of the graph, i.e. up to density $\rho \sim 50$, represents the free phase of traffic, while the second part reproduces the congested phase.

Here we show the evolution in time, starting by a network initially empty, of car density within a day from 6:00 to 10:00, as depicted in Figs. 40–44, and from 16:00 to 20:00, as showed by Figs. 45–49 at different hours. See [6] for animations.

Figure 42 reveals the formation of a queue which enters the road propagating backwards, as indicated by Figs. 43 and 44. Another shock propagating backwards along the road can be observed in Figs. 47 and 48, which is later absorbed as showed by Fig. 49.

5 Conclusions

An elaboration and an implementation of Godunov method and of kinetic schemes even extended to second order provided numerical solutions to the problem of traffic flows on road networks. Since along the roads the schemes present the same features as for conservation laws, the new and original aspect is given by the treatment of the solution at junctions. Our tests show the effectiveness of the approximations, revealing that kinetic schemes of 3-velocities are more accurate than Godunov scheme.

Acknowledgements The authors would like to thank Antonino Sgalambro for his assistance with the computational work.

References

1. Aregba-Driollet D, Milišić V (2004) Kinetic approximation of a boundary value problem for conservation laws. Numer Math 97:595–633
2. Aregba-Driollet D, Natalini R (2000) Discrete kinetic schemes for multidimensional systems of conservation laws. SIAM J Numer Anal 37(6):1973–2004
3. Astarita V (2002) Node and link models for network traffic flow simulation. Math Comput Model 35:643–656
4. Bardos C, Le Roux AY, Nédélec JC (1979) First order quasilinear equation with boundary conditions. Commun Partial Differ Equ 4:1017–1034
5. Bressan A (2000) Hyperbolic systems of conservation laws. The one-dimensional Cauchy problem. Oxford lecture series in mathematics and its applications, vol 20. Oxford University Press
6. Bretti G, Sgalambro A http://www.iac.rm.cnr.it/ bretti/TrafficNumericalSolution.html
7. Bretti G, Natalini R, Piccoli B (2006) Numerical approximations of a traffic flow model on networks. Netw Heterog Media 1(1):57–84
8. Chitour Y, Piccoli B (2005) Traffic circles and timing of traffic lights for cars flow. Discret Continuous Dyn Syst Ser 5:599–630
9. Coclite GM, Garavello M, Piccoli B (2005) Traffic flow on a road network. SIAM Math Anal 36:1862–1886
10. Dafermos CM (2000) Hyperbolic conservation laws in continuum physics. Grundlehren der Mathematischen Wissenschaften, vol 325. Springer, Berlin
11. Deshpande SM (1986) A second order accurate, kinetic-theory based, method for inviscid compressible flows. NASA Langley Tech, Paper 2613
12. Godlewski E, Raviart PA (1991) Hyperbolic systems of conservation laws. Mathématiques & applications [Mathematics and applications], vol 3/4. Ellipses, Paris
13. Godunov SK (1959) A finite difference method for the numerical computation of discontinuous solutions of the equations of fluid dynamics. Mat Sb 47:271–290
14. Haberman R (1977) Mathematical models. Prentice-Hall, New Jersey, pp 255–394
15. Harten A, Lax PD, van Leer B (1983) On upstream differencing and Godunov type schemes for hyperbolic conservation laws. SIAM Rev 25:35–61
16. Holden H, Risebro NH (1995) A mathematical model of traffic flow on a network of unidirectional roads. SIAM J Math Anal 26:999–1017
17. Jin S, Xin Z (1995) The relaxation schemes for systems of conservation laws in arbitrary space dimensions. Commun Pure Appl Math 48(3):235–276
18. Klar A (2002) Kinetic and macroscopic traffic flow models. In: Lecture notes for the XX school of computational mathematics, "Computational aspects in kinetic models", Piano di Sorrento (Italy), September 22–28
19. Leveque RJ (2002) Finite volume methods for hyperbolic problems. Cambridge texts in applied mathematics. Cambridge University Press
20. Lighthill MJ, Whitham GB (1955) On kinematic waves. II. A theory of traffic flow on long crowded roads. Proc Roy Soc Lond Ser A 229:317–345
21. Natalini R (1998) A discrete kinetic approximation of entropy solutions to multidimensional scalar conservation laws. J Differ Equ 148:292–317
22. Perthame B (1990) Boltzmann type schemes for gas dynamics and the entropy property. SIAM J Numer Anal 27(6):1405–1421
23. Perthame B (2002) Kinetic formulation of conservation laws. Oxford lecture series in mathematics and its applications, Oxford
24. Richards PI (1956) Shock waves on the highway. Oper Res 4:42–51
25. Whitham GB (1974) Linear and nonlinear waves. Pure and applied mathematics. A Wiley-Interscience series of texts, monographs, and tracts. Wiley, New York